Brain Research Unit, O.V. Lounasmaa Laboratory

Cortical rhythms as markers of neural processing

Hannu Laaksonen

Aalto University

DOCTORAL DISSERTATIONS

Aalto University publication series
DOCTORAL DISSERTATIONS 119/2012

Cortical rhythms as markers of neural processing

Hannu Laaksonen

A doctoral dissertation completed for the degree of Doctor of Science in Technology to be defended, with the permission of the Aalto University School of Science, at a public examination held at the Auditorium F239 at the Aalto University on 10th of October 2012 at 12.

Aalto University
School of Science
O.V. Lounasmaa Laboratory
Brain Research Unit

Supervising professors
Prof. Ari Koskelainen
Department of Biomedical Engineering and Computational Science
School of Science, Aalto University
Finland

Thesis advisors
Acad. Prof. Riitta Salmelin
Brain Research Unit, O.V. Lounasmaa Laboratory
School of Science, Aalto University
Finland

Preliminary examiners
Dr. Kimmo Uutela
GE Healthcare
Finland

Dr. Ole Jensen
Centre for Cognitive Neuroimaging
Donders Institute for Brain, Cognition and Behaviour
Radboud University Nijmegen
The Netherlands

Opponents
Dr. Gareth Barnes
Wellcome Trust Centre for Neuroimaging
University College London
United Kingdom

Aalto University publication series
DOCTORAL DISSERTATIONS 119/2012

ISBN 978-952-60-4786-7 (printed)
ISBN 978-952-60-4787-4 (pdf)
ISSN-L 1799-4934
ISSN 1799-4934 (printed)
ISSN 1799-4942 (pdf)
http://urn.fi/URN:ISBN:978-952-60-4787-4

Unigrafia Oy
Helsinki 2012

Finland

441 697
Printed matter

Author
Hannu Laaksonen

Name of the doctoral dissertation
Cortical rhythms as markers of neural processing

Publisher School of Science

Unit O.V. Lounasmaa Laboratory

Series Aalto University publication series DOCTORAL DISSERTATIONS 119/2012

Field of research Engineering Physics, Biomedical Engineering

Manuscript submitted 1 June 2012 **Date of the defence** 10 October 2012

Permission to publish granted (date) 16 August 2012 **Language** English

☐ **Monograph** ☒ **Article dissertation (summary + original articles)**

Abstract

Magnetoencephalography (MEG) is an excellent tool for noninvasive investigation of neuronal activity from outside of the head. It provides millisecond temporal accuracy and good spatial resolution. The classical measure of task-related brain activity is the evoked response that is phase-locked to task or stimulus. But the brain also exhibits spontaneous oscillations, or rhythmic activity, that has been observed to be modulated during task or in response to stimuli.

This Thesis mainly focuses on investigations of cortical brain rhythms, developing methods for analyzing them and probing their relationship with evoked responses. While the sensor level MEG signal can be used successfully for studying evoked responses and cortical rhythmic activity, a proper evaluation of the data requires localization of the active brain areas. For this purpose, a beamforming technique called Dynamic Imaging of Coherent Sources (DICS) was used and modified in this Thesis. With DICS, it is possible to examine both power level modulations of rhythmic activity and functional connectivity between different brain regions conveyed by rhythmic activity.

In this Thesis, an event-related version of a beamformer method DICS was implemented to assist the modeling of rhythmic activity. The feasibility of this new method, erDICS, was shown with simulations and real MEG data. The method was further applied to compare evoked responses and rhythmic activity in a high-level cognitive task of picture naming, with the conclusion that the two measures of cortical processes are largely detached and that both measures are needed for an accurate portrayal of brain activity. With another data set from a word priming study, erDICS was used to investigate connections between the left superior temporal cortex and other cortical regions. The method revealed different brain networks for phonological and semantic priming.

Keywords magnetoencelography, MEG, rhythms, oscillations, evoked response, functional connectivity

ISBN (printed) 978-952-60-4786-7 **ISBN (pdf)** 978-952-60-4787-4

ISSN-L 1799-4934 **ISSN (printed)** 1799-4934 **ISSN (pdf)** 1799-4942

Location of publisher Espoo **Location of printing** Helsinki **Year** 2012

Pages 70 **urn** http://urn.fi/URN:ISBN:978-952-60-4787-4

A? Aalto-yliopisto

Tiivistelmä

Aalto-yliopisto, PL 11000, 00076 Aalto www.aalto.fi

Tekijä
Hannu Laaksonen

Väitöskirjan nimi
Aivokuoren rytmit hermostollisen käsittelyn merkkinä

Julkaisija Perustieteiden korkeakoulu

Yksikkö O.V. Lounasmaa -laboratorio

Sarja Aalto University publication series DOCTORAL DISSERTATIONS 119/2012

Tutkimusala Teknillinen fysiikka, lääketieteellinen tekniikka

Käsikirjoituksen pvm 01.06.2012 **Väitöspäivä** 10.10.2012

Julkaisuluvan myöntämispäivä 16.08.2012 **Kieli** Englanti

☐ **Monografia** ☒ **Yhdistelmäväitöskirja (yhteenveto-osa + erillisartikkelit)**

Tiivistelmä

Magnetoenkefalografia (MEG) on erinomainen työkalu aivojen toiminnan tutkimiseen pään ulkopuolelta. Se mahdollistaa aivosignaalien mittauksen millisekunttien aikatarkkuudella ja hyvällä paikkatarkkuudella. Perinteisesti tehtäväsidonnaista aivotoimintaa on tutkittu tehtävään tai ärsykkeeseen vaihelukittuneilla herätevasteilla. Aivot tuottavat myös spontaaneja rytmejä, joiden on havaittu vaihtelevan tehtävän aikana tai ärsykkeen seurauksena.

Tämä väitöskirja keskittyy aivokuoren rytmiseen toimintaan, sen tutkimiseen tarvittavien menetelmien kehittämiseen ja rytmien ja herätevasteiden välisen yhteyden tarkasteluun. Vaikka anturitason MEG-signaalia voidaan käyttää menestyksekkäästi herätevasteiden ja rytmien tutkimiseen, niiden perusteellinen tarkastelu vaatii myös tietoa aktiivisten aivoalueiden paikoista. Tätä varten väitöskirjassa käytettiin Dynamic Imaging of Coherent Sources (DICS) -menetelmää, jonka avulla on mahdollista tutkia sekä rytmisen toiminnan tehon muokkautumista eri aivoalueilla että toiminnallista kytkeytyvyyttä aivoalueiden välillä.

Väitöskirjassa kehitettiin tehtäväsidonnainen versio DICS:stä (event-related DICS, erDICS) rytmisen toiminnan mallintamisen avuksi. Menetelmän käyttökelpoisuutta testattiin simuloidun ja oikean MEG-datan avulla. Uutta menetelmää sovellettiin herätevasteiden ja rytmisen toiminnan vertailuun useita aivoalueita aktivoivassa kokeessa, jossa koehenkilöt nimesivät kuvia. Loppupäätelmänä oli, että nämä kaksi aivokuoren aktivaation mittaria ovat pitkälti eriävät ja molempia tarvitaan aivojen toiminnan kokonaisuuden hahmottamiseksi. Toisessa kokeessa, jossa tutkittiin sanalistojen ns. priming-vaikutusta (virittäminen), erDICS:ia käytettiin toiminnallisen kytkeytyvyyden tutkimiseen. Menetelmä paljasti erilaiset aivoverkot äänneasun ja merkityksen virittämisessä.

Avainsanat Magnetoenkefalografia, MEG, rytmit, funktionaalinen kytkeytyvyys

ISBN (painettu) 978-952-60-4786-7 **ISBN (pdf)** 978-952-60-4787-4

ISSN-L 1799-4934 **ISSN (painettu)** 1799-4934 **ISSN (pdf)** 1799-4942

Julkaisupaikka Espoo **Painopaikka** Helsinki **Vuosi** 2012

Sivumäärä 70 **urn** http://urn.fi/URN:ISBN:978-952-60-4787-4

Preface

This Thesis was carried out in the Brain Research Unit of the O.V. Lounasmaa Laboratory, Aalto University, and was financially supported by the Academy of Finland, Sigrid Jusélius Foundation, Finnish Foundation for Technology Promotion, Emil Aaltonen Foundation and Finnish Funding Agency for Technology and Innovation.

I would like to thank my instructor, Acad. Prof. Riitta Salmelin, for her guidance and support throughout my thesis work. Her passion for science and scrupulous attitude towards work have been truly inspiring for me. Riitta, you have been the real force behind this work.

The director of the Brain Researh Unit, Prof. Riitta Hari, has made a tremendous work in building and maintaining a world class research unit. This Thesis would not exist without her efforts. I also wish to thank Prof. Mikko Paalanen, the former director of the Low Temperature Laboratory, for inviting me to a job interview all those years ago when I was still just a master's student at the Helsinki University of Technology. This started my journey that eventually led to the publication of this Thesis.

This work would not have been possible without the effort of my co-authors. Sincerest thanks to Dr. Jan Kujala, Mr. Timo Saarinen, Dr. Annika Hultén, Dr. Mia Liljeström, Dr. Johanna Vartiainen, Dr. Tiina Parviainen, Prof. Matti Laine and Dr. Minna Vihla. I am grateful to my preliminary examiners Dr. Kimmo Uutela and Dr. Ole Jensen for their work and comments on this Thesis and to my follow-up group, Dr. Uutela and Doc. Jyrki Mäkelä, for their valuable observations. I would like to thank Dr. Catherine Nangini for kindly checking the language of this Thesis.

Working in the Brain Research Unit has been a pleasure and a privilege.

The warm, unique atmosphere has been created by a mix of talented, kind and bright students, postdocs, senior scientists, technical personnel and secretaries. You are far too many to mention by name, but you are all deeply appreciated. Specifically I would like to thank my past roommates Lauri, Miiu, Liisa, Pavan and Hanna for their friendship during these years and the English course members Johanna and Annika for many memorable moments. Also, my floorball teammates are highly appreciated for making Tuesday the best day of the week.

I have been lucky enough to have a circle of important close friends, who have reminded that there is actually life outside the red walls of BRU: Juha, Janne and Jere all the way back from the Hyvinkää days and Arto, Teemu, Missu and Päivi whom I had the pleasure of meeting during my studies. Your friendship is very important to me.

I wish to thank my parents, Erkki and Tarja, for always being there to support and encourage me. And huge thanks to my brother Timo.

And finally, I wish to express my gratitude to Lotta, for her love through the good and bad times. Thank you for everything.

Espoo, September 12, 2012,

Hannu Laaksonen

Contents

List of Publications

This thesis consists of an overview and of the following publications which are referred to in the text by their Roman numerals.

I Saarinen, T., **Laaksonen, H.**, Parviainen, T., and Salmelin, R. Motor cortex dynamics in visuomotor production of speech and non-speech mouth movements. *Cerebral Cortex*, 16, p. 212-222, 2006.

II Laaksonen, H., Kujala, J., and Salmelin, R. A method for spatiotemporal mapping of event-related modulation of cortical rhythmic activity. *Neuroimage*, 42, p. 207-217, 2008.

III Hultén A., **Laaksonen, H.**, Vihla M., Laine M., and Salmelin R. Modulation of brain activity after learning predicts long-term memory for words. *Journal of Neuroscience*, 30, p. 15160-15164, 2010.

IV Laaksonen, H., Kujala J., Hultén A., Liljeström M., and Salmelin R. MEG evoked responses and rhythmic activity provide spatiotemporally complementary measures of neural activity in language production. *Neuroimage*, 60, p. 29-36, 2012.

V Kujala J., Vartiainen J., **Laaksonen, H.**, and Salmelin R. Neural interactions at the core of phonological and semantic priming of written words. Accepted for publication in *Cerebral Cortex*, 2012.

Author's Contribution

Publication I: "Motor cortex dynamics in visuomotor production of speech and non-speech mouth movements"

I acquired the MEG data together with the first author, took part in data analysis and actively participated in the writing of the manuscript.

Publication II: "A method for spatiotemporal mapping of event-related modulation of cortical rhythmic activity"

I developed new analysis tools based on a previously implemented beamforming method. I performed the necessary simulations and analyzed the simulated and real MEG data with the new method. I was the first author in this study and wrote the manuscript with input from my co-authors.

Publication III: "Modulation of brain activity after learning predicts long-term memory for words"

I contributed to and advised in the practical data analysis and statistical testing of the results. I actively participated in the writing of the manuscript.

Publication IV: "MEG evoked responses and rhythmic activity provide spatiotemporally complementary measures of neural activity in language production"

I implemented the needed tools for the analysis of rhythmic activity and carried out the data analysis. I was the first author in this study and wrote the manuscript with input from my co-authors.

Publication V: "Neural interactions at the core of phonological and semantic priming of written words"

I took part in the development of the analysis tools used in the study and actively participated in the writing of the manuscript.

List of Abbreviations

AP	Action Potential
BEM	Boundary Element Model
CFC	Cross-Frequency Coupling
CSD	Cross-Spectral Density
DICS	Dynamic Imaging of Coherent Sources
ECD	Equivalent Current Dipole
EEG	Electroencephalography
EMG	Electromyography
EOG	Electro-Oculography
FFT	Fast Fourier Transform
fMRI	Functional Magnetic Resonance Imaging
HPI	Head Position Indicator
LCMV	Linearly Constrained Minimum Variance
M1	Primary Motor Cortex
MCE	Minimum Current Estimate
MEG	Magnetoencephalography
MNE	Minimum Norm Estimate
PLV	Phase-Locking Value
PSP	Postsynaptic Potential
SAM	Synthetic Aperture Magnetometry

SI	Synchronization index
SMC	Sensorimotor Cortex
SNR	Signal-to-Noise Ratio
SQUID	Superconducting Quantum Interference Device
SSP	Signal Space Projection
SSS	Signal Space Separation

1. Introduction

Studying the human brain is one of the most intriguing research fields of today. The task is daunting, however, as the sheer complexity of the nervous system makes the pursuit extremely convoluted. The basic units of the human brain, neurons, number in the order of 10^{11} and the connections between them at a staggering 10^{14} – prior to 64-bit computing it would not have been even possible to map so many indices. The upper limit of a 32-bit address space is roughly only $4 \cdot 10^9$, which is also the number of possible unique IPv4 addresses. Due to the complicated nature of the brain, it cannot be investigated in all its aspects at once and the research field is thus split into several subfields. The functions of the nervous system can be approached through anatomical or behavioral observations and measurements. To actually see what goes on inside the skull when the brain is in action, we need instruments for measuring activity from single or a few neuronal cells, or even imaging the whole functioning brain at once. No single approach gives us all of the answers, but by putting together the various pieces we get closer to understanding how the nervous system works.

Magnetoencephalography (MEG) is an excellent tool for noninvasive investigation of neuronal activity from outside of the head. It provides millisecond temporal accuracy and good spatial resolution. The classical measure of task-related brain activity is the evoked response that is phase-locked to task or stimulus. But the brain also exhibits spontaneous oscillations, or rhythmic activity, that has been observed to be modulated during a task or in response to stimuli.

This Thesis mainly focuses on investigations of cortical brain rhythms, developing methods for analyzing them and probing their relationship with evoked responses. While the sensor-level MEG signal can be used suc-

cessfully for studying evoked responses and cortical rhythmic activity, a proper evaluation of the data requires localization of the active brain areas. For this purpose, a beamforming technique called Dynamic Imaging of Coherent Sources (DICS) was used and modified into an event-related variant (erDICS) in this Thesis. With DICS, it is possible to examine both power-level modulations of rhythmic activity and functional connectivity between different brain regions conveyed by rhythmic activity.

The next chapter of this Thesis will briefly describe the basics of neuronal signal generation and the physics and instrumentation of MEG; for a more detailed account, one may consult, e.g., the review article by Hämäläinen et al. (1993) or the textbook by Hansen et al. (2010). Chapter 3 outlines the main aims of this Thesis, and Chapter 4 describes the main results of the separate studies. Chapter 5 discusses the main findings and future directions.

2. Background

2.1 Origin of the MEG signals

2.1.1 The brain

The human brain is customarily divided into three parts: the cerebrum, cerebellum and brain stem. The cerebrum and cerebellum can further be divided into left and right hemispheres. The outer part of the cerebrum is called the cerebral cortex and it plays a key role in human awareness and consciousness. Roughly every tenth, or 10^{10}, of human neurons are found in the cerebral cortex. This layer is only a few millimeters thick and is heavily folded so that most of its surface is hidden in sulci. Folded out, it would cover the area of 2500 cm^2, the same as a large cloth napkin. In MEG studies, the main focus is on the cerebral cortex. This is because of its functional role in many cognitive functions and because, as it is the outmost layer of the cerebrum, MEG measurement systems can most readily pick up signals from this part of the brain.

The cerebral cortex in both of the hemispheres is often divided topographically into four lobes: the occipital lobe, parietal lobe, temporal lobe and frontal lobe (Figure 2.1). A major landmark, the central sulcus or Rolandic fissure, separates the frontal and parietal lobes and another major sulcus, the lateral sulcus or Sylvian fissure, separates the frontal lobe from the temporal lobe. Relative directions in the brain are, by convention, posterior (towards the back of the head), anterior (towards the front of the head), superior/inferior (above/below) and lateral/medial (towards the sides or the midline).

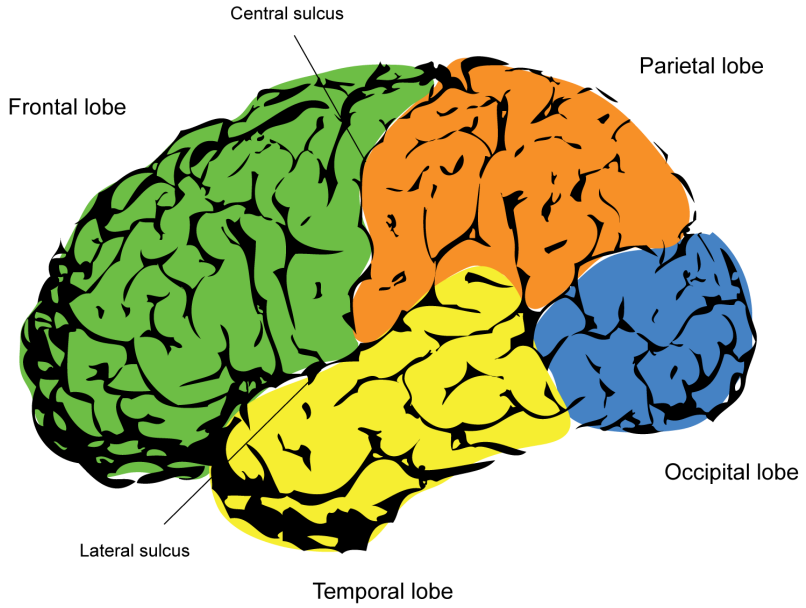

Figure 2.1. Schematic illustration of the brain (left hemisphere).

The cortex may also be divided according to the different functional roles associated with different areas. For example, the primary motor area that controls execution of movements is located anterior to the central sulcus; posterior to that sulcus lies the primary somatosensory area that processes touch. The main visual processing area is located in the occipital cortex, the most posterior part of the brain. Most connections from the peripheral nervous system connect to the opposite (contralateral) side of the brain. Therefore, when, for example, a subject moves his/her right hand, the most prominent activation is observed in the left sensorimotor cortex. There are also connections to the same side (ipsilateral), which results in bilateral activity.

2.1.2 Neurons and synapses

The basic information processing unit in the human brain is a neuronal cell or a neuron. Neurons exchange information among themselves via an electric and chemical signaling system. A single neuron consists of a cell body, or soma, a number of information-receiving dendrites and an axon, which transmits signal to other neurons. The connecting junction between an axon of one neuron and a dendrite of another is called a synapse. The signal travels in the form of electric potential change along the neuron cell membrane, but is delivered chemically to the next neuron at the synapse.

This arrangement combines fast information transfer (electric potential) with the possibility of large-scale modulation (chemical signals).

At rest, a neuron's cell membrane potential is around -70 mV, which is created by a concentration gradient of various ions across the cell membrane and is maintained by the different membrane permeabilities to different ions and active ion pumps. When the cell receives excitatory input from the numerous synapses in its dendrites, the soma depolarizes (making it more positive). If the soma depolarizes above around -55 mV, it kicks off an event called an action potential (AP) which travels along the axon using voltage-gated ion channels. During an action potential, only a small patch of the axon is affected at a time. At first, the Na^+ channels open, bringing Na^+ ions into the cell and strongly depolarizing the cell membrane. After a delay, this is followed by repolarization via closing of the Na^+ channels and opening of the K^+ channels that bring the cell back to the resting level. The whole event only lasts for a few milliseconds, but causes the neighboring cell membrane to depolarize and start the same cycle. This causes an action potential to travel as an electric pulse from the soma to the end of the axon. After the AP moves on, the cell membrane goes into a refractory state for about a millisecond. During this time, no action potential can be formed, ensuring that action potentials always travel only in one direction.

When the action potential reaches the synapse, the presynaptic neuron releases neurotransmitters into the cleft between the pre- and postsynaptic neuron (Figure 2.2). In an excitatory synapse, the neurotransmitters cause the postsynaptic neuron to depolarize locally, initiating a postsynaptic potential (PSP). The PSPs arriving at different dendritic synapses of the postsynaptic neuron sum both spatially and temporally. If the potential at the soma reaches high enough a level, a new AP will be generated at the axon hillock of the postsynaptic neuron. Inhibitory synapses have the opposite effect. They either hyperpolarize or increase conductance of the cell membrane without changing the cell membrane potential, making it more difficult for the membrane potential to reach the threshold for AP generation.

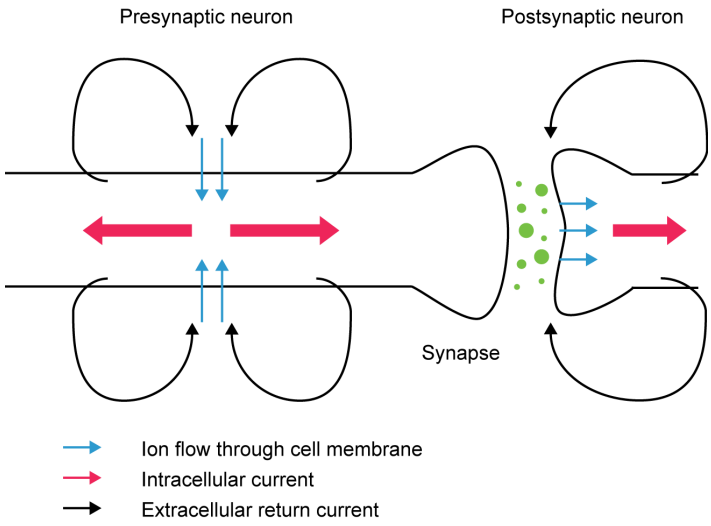

Figure 2.2. Schematic illustration of the neuronal currents: action potential in the presynaptic neuron and postsynaptic currents in the postsynaptic neuron.

2.1.3 External fields due to neuronal currents

Neuronal activity produces currents, which generate electromagnetic fields that can be measured with imaging modalities such as MEG and EEG. As described above, there are two sources of neuronal activity: action potentials and postsynaptic potentials. When measuring brain activity with MEG and EEG, we mostly observe only one of them, the PSP. The reasons are three-fold: field decay, spatial summation and temporal summation.

The field produced by APs can be viewed as quadrupolar (the intracellular current is flowing in two directions from the site of an AP), which decays as $1/r^3$, where r denotes the distance from the site. In the case of PSP, however, where the source of the field can be viewed as a dipole (current flowing into one direction only), which decays as $1/r^2$ and thus persists over longer distances.

It has been shown that most of the MEG/EEG signal is generated in the pyramidal cells of the cortex (Okada et al. 1997). The apical dendrites of this type of large neuron are aligned in parallel. Therefore, when several neurons in the same region receive a signal, the PSPs sum spatially, making it easier to measure the neuronal signal outside of the head.

The characteristic lifetime of a PSP is on the order of ten milliseconds,

whereas an AP lasts only for around one ms. This makes it possible for several PSPs to sum temporally, but APs would have to be extremely synchronized to have that benefit. Typically, it takes on the order of thousands nearly simultaneous, spatially-close PSPs to generate an electromagnetic field strong enough to be detected from the outside of the head.

It is important to note that the pyramidal cells are oriented perpendicular to the cortical surface. Because the cortex is heavily folded and forms gyri and sulci, this means that the neural currents in the crown of the gyri are oriented radial to the skull whereas the neural currents generated in the walls of sulci are aligned parallel to the skull (Figure 2.3). This has important implications when measuring the signal with MEG, as MEG is particularly sensitive to currents tangential to the skull and less to radial currents (more on this in section 2.4.1). Importantly, about 2/3 of the cortex surface is in the fissural cortex (Henery and Mayhew 1989).

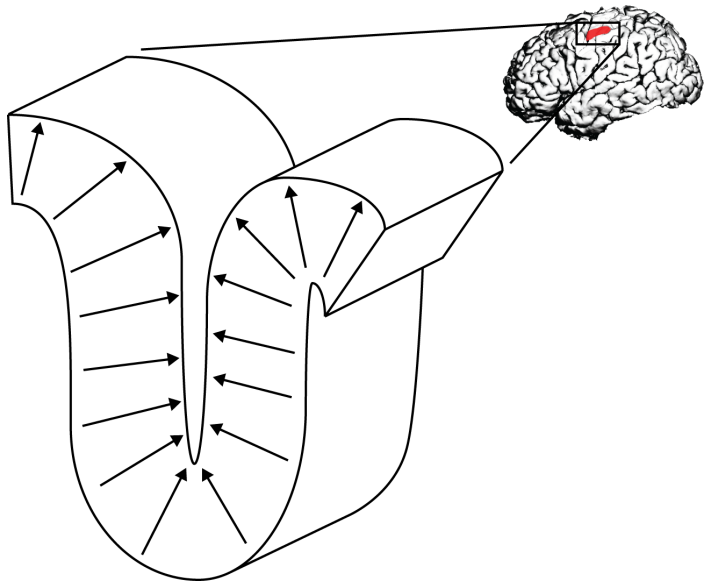

Figure 2.3. Orientation of the PSP current flow in different parts of a gyrus/sulcus.

2.2 MEG measurement device

Magnetic fields generated by the human brain were recorded for the first time in 1968 using a simple magnetometer (Cohen 1968). However, practical measurements of magnetic signals outside the head became possible only after the introduction of the superconducting quantum interference

device (SQUID) (Zimmerman and Silver 1966; Zimmerman et al. 1970; Cohen 1972).

A SQUID is a superconducting ring with one or two weak links called Josephson junctions (Josephson 1962). When a bias current is applied to such a loop, its output varies periodically according to the magnetic flux that passes through the SQUID loop. This output can be set to zero with a feedback current, such that the change in the magnetic flux induces a change in the feedback current. In this type of arrangement, the feedback current is proportional to the magnetic flux and enables detection of extremely small changes in magnetic field.

A typical SQUID is very small and would by itself be quite insensitive to an external magnetic field. In MEG, the sensitivity of signal detection is enhanced by using a separate larger pick-up coil that is then coupled to the smaller SQUID loop with a signal coil. The properties of the pick-up coil determine the manner in which the device detects the magnetic field. Typical pick-up coil types are magnetometers and gradiometers. A magnetometer is a single loop that detects field components normal to its surface. A gradiometer consists of two loops wound in opposite directions such that their output is sensitive to the spatial field change at the loop location. If the two opposing coils are in the same plane, this coil setup is called a planar gradiometer and if they are on the same axis, the setup is called an axial gradiometer (Figure 2.4).

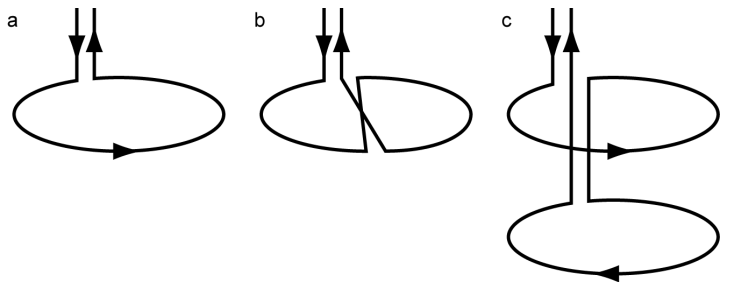

Figure 2.4. Different types of pick-up coils. (a) A magnetometer is a single loop. (b) A planar gradiometer consists of two loops on the same plane and (c) an axial gradiometer has two loops, one on top of the other.

If a source is far away from the pick-up coil, gradiometers tend to miss it, because the spatial derivative of the field diminishes with distance. Magnetometers, on the other hand, are more sensitive to far away sources as they measure the field itself. However, this also makes them more prone to disturbance from external sources, whereas gradiometers can

better detect local field changes. If a dipolar current is located fairly close to the MEG sensors, a planar gradiometer will give a maximal signal on top of the source current and a magnetometer on both sides of it.

All the data examined in this Thesis were collected using a 306-channel Neuromag Vectorview™ MEG device manufactured by Elekta Oy, Helsinki, Finland. It contains 102 sensor elements in a helmet covering the head. Each sensor element contains two orthogonal planar gradiometers and one magnetometer. Only signals recorded with the planar gradiometers were used in this Thesis, because of their better signal-to-noise ratio (SNR) and more accurate spatial information already at the sensor level.

Besides the MEG signal, eye movements are typically recorded with electrodes attached to the skin close to the subject's eyes (electro-oculography, EOG). An eye blink or saccade produces a large artifact in the MEG signal, and intervals contaminated by such movements are typically removed from the data analysis. If needed, subjects' muscle activity can be recorded with electrodes attached to the relevant part of the skin (electromyography, EMG).

The position of the head relative to the sensor array can be determined using small head position indicator (HPI) coils that are typically attached to the forehead and behind the ears. The location of these coils may be determined by briefly feeding a current into them and localizing them based on the resulting magnetic field. By further defining the HPI coil locations with respect to anatomical landmarks (nasion, preauricular points), using a 3D digitizer, the MEG source-level results may be displayed on structural magnetic resonance images of the subjects' brains.

The magnetic fields generated by neuronal activity are very weak. The Earth's magnetic field is over 10^8 times stronger than the measured signal (Hämäläinen et al. 1993) and even passing cars on the street, electric noise from wirings and normal laboratory equipment can interfere with the measurements. Therefore, there is a need for suppression of ambient and electronic noise. This can be achieved in multiple ways.

First, an MEG device is placed in a magnetically shielded room that reduces external fields via passive shielding, in some cases assisted by an active compensation system. Second, the choice of measurement coils is important. Using gradiometers reduces the amount of outside interfer-

ence, as far-away fields will be locally homogeneous and thus cancel out. Third, noise can be reduced with computational methods, such as signal space projection (SSP, Uusitalo and Ilmoniemi 1997) and signal space separation (SSS, Taulu et al. 2004). In SSP, an interference field estimated from an empty room measurement is projected out from the measured data. In SSS, the signal is separated into two subspaces, one originating from the inside of the measurement helmet and one originating from the outside.

2.3 Evoked responses and rhythmic activity

In a traditional MEG study, a certain type of task or stimulus is repeated multiple times, and MEG data averaged over these repeats, or trials, are used to estimate the underlying neural activity. Averaging improves the SNR by reducing the contribution of noise uncorrelated to the task. The response to a single stimulus usually has an insufficient SNR for reliable analysis. These phase-locked evoked responses are typically evident within 1 s of the stimulus or task onset. In simple sensory and motor tasks, evoked responses arise from the sensory and motor representation areas, but in more demanding cognitive tasks, evoked responses are generated in many other areas as well, throughout the cortex (Brenner et al. 1975; Brenner et al. 1978; Hari et al. 1980; Salmelin et al. 1994; Helenius et al. 1998; Salmelin 2007).

Apart from the evoked responses, cortical rhythms are the most prominent aspect of brain activity recorded with EEG/MEG. In fact, the first published EEG recording reported 10-Hz brain oscillations over the posterior brain regions (Berger 1929). This well-know rhythm is commonly called the alpha rhythm and, subsequently, Greek letters have been given as names to several other distinct brain rhythms, as classified by their region of origin and frequency content. The mu rhythm in the rolandic region has a typical comb-like shape, with spectral peaks around 7-13 and 16-24 Hz (Gastaut 1952; Hari and Salmelin 1997). Beta waves (13-35 Hz) are recorded over the motor cortex (Hari and Salmelin 1997). The theta rhythm (3-8 Hz, Ishii et al. 1999; Jensen and Tesche 2002) is seen in the frontal brain regions and the tau rhythm (around 8 Hz) around the auditory cortex (Niedermeyer 1990; Tiihonen et al. 1991). Gamma band activity (30-100 Hz) has been reported over several cortical areas

(Tallon-Baudry et al. 1997; Singer 1999; Fries et al. 2001), although most studies seem to focus on the occipital cortex (e.g., Hoogenboom et al. 2006; Muthukumaraswamy et al. 2010).

The occipito-parietal alpha rhythm is most prominent when the subject is awake with the eyes closed and is decreased when the subject is presented with a visual stimulus or during visual imagery (Salenius et al. 1995; Hari and Salmelin 1997). This rhythm seems to be suppressed more strongly by a more intense task, as observed, e.g., when comparing brain responses between passive viewing of pictures and naming of the same pictures, either silently or aloud (Salmelin et al. 1994). Modulation of the alpha rhythm is not limited to sensory events; e.g., an increase in parieto-occipital 10-Hz rhythm has been linked to memory load (Jensen et al. 2002; Tuladhar et al. 2007).

The mu rhythm is suppressed by limb movements and tactile stimulation (as reviewed, e.g., by Hari and Salmelin 1997), followed by a rebound above baseline level after the movement offset. This rebound has been suggested to reflect cortical inactivation or immobilization when returning to rest (Salmelin et al. 1995; Chen et al. 1998; Pfurtscheller and Lopes da Silva 1999). The rebound of the 20-Hz component of the mu rhythm seems to be faster and stronger than the rebound of the 10-Hz component (Pfurtscheller 1981; Salmelin and Hari 1994b). At rest, the mu rhythm is mostly visible only close to the hand representation area in the motor cortex (Salmelin and Hari 1994a).

It is common to divide brain rhythms into two categories; spontaneous and induced. Spontaneous rhythms are observed without any external stimulus or task and induced rhythms are observed in response to a stimulus or task. For example, the occipital alpha rhythm, occurring when the subject's eyes are closed, belongs to the category of spontaneous rhythms and an increase of the 20-Hz rhythms in the motor cortex after limb movement (e.g. Salmelin and Hari 1994b) is seen as modulation of induced rhythmic activity.

A very striking difference between evoked responses and brain oscillations is the duration of the events. Evoked responses are typically rapid transient events (< 1 s in a typical MEG experiment), while rhythms last over several seconds. This extended temporal scale of oscillatory activity has been suggested to be useful in processing sequential events by keep-

ing information available over longer time scales (Dinse et al. 1997).

2.4 Source modeling and data analysis

While the sensor level MEG signal can be successfully used for studying evoked responses and cortical rhythmic activity, several distinct brain regions can contribute to the measurements and confound the data analysis. In order to properly separate signals from different sites, it is therefore vital to be able to go from measurements outside the head to modeling the neural currents inside the brain. This decomposition of the measured signal is called solving the inverse problem, and it usually requires some assumptions about the brain's geometry and current distribution.

2.4.1 Forward model

Before solving the inverse problem, one must first solve the forward problem, i.e. estimating the measurements if the current density in the brain were known. This problem can be solved starting from Maxwell's equations

$$\nabla \cdot \mathbf{E} = \rho/\varepsilon_0, \tag{2.1}$$

$$\nabla \times \mathbf{E} = -\partial \mathbf{B}/\partial t, \tag{2.2}$$

$$\nabla \cdot \mathbf{B} = 0, \tag{2.3}$$

$$\nabla \times \mathbf{B} = \mu_0(\mathbf{J} + \varepsilon_0 \partial \mathbf{E}/\partial t), \tag{2.4}$$

where $\mathbf{E}$ is the electric field, ρ is the charge density, ε_0 is the permittivity of vacuum, $\mathbf{B}$ is the magnetic field, μ_0 is the vacuum permeability and $\mathbf{J}$ is the total current density. Here the permeability of the head is assumed to be that of vacuum.

Because neuronal events are slow, with typical frequencies below 100 Hz, we can use the quasi-static approximation of Maxwell's equations (Hämäläinen et al. 1993). This renders the time derivates in Eq. 2.3 and Eq. 2.4 equal to zero. The magnetic field satisfying Eq. 2.2 - 2.4 can then be calculated with Ampère-Laplace's law as

$$\mathbf{B}(\mathbf{r}) = \frac{\mu_0}{4\pi} \int \frac{\mathbf{J}(\mathbf{r}') \times (\mathbf{r} - \mathbf{r}')}{\mid \mathbf{r} - \mathbf{r}' \mid^3} dv', \tag{2.5}$$

where $\mathbf{B}$ is the magnetic field outside the head at location $\mathbf{r}$ and $\mathbf{J}(\mathbf{r}')$ is the current density at point $\mathbf{r}'$ inside the brain.

The current density is typically divided into macroscopic volume current $\mathbf{J_v}$ and primary current $\mathbf{J_p}$. The primary current is the neuronal current flowing inside the cell and the volume current is the passive current flowing in the conducting medium. Volume currents are driven by the macroscopic electric field $\mathbf{E}$ and obey Ohm's law. Current density can therefore be denoted as

$$\mathbf{J} = \mathbf{J_p} + \mathbf{J_v} = \mathbf{J_p} + \sigma\mathbf{E} = \mathbf{J_p} - \sigma\nabla V, \tag{2.6}$$

where σ is the conductivity of the medium and V is the electric potential.

Using Eq. 2.2 – 2.6, it is now possible to write out equations for the magnetic field outside the head and the relationship between V and the primary current:

$$\mathbf{B}(\mathbf{r}) = \frac{\mu_0}{4\pi}\int (\mathbf{J_p}(\mathbf{r}') + V\nabla'\sigma) \times \frac{\mathbf{r}-\mathbf{r}'}{\mid \mathbf{r}-\mathbf{r}' \mid^3} dv' \tag{2.7}$$

$$\nabla \cdot (\sigma\nabla V) = \nabla \cdot \mathbf{J_p}. \tag{2.8}$$

See Sarvas (1987) and Hämäläinen et al. (1993) for more details. By solving V from Eq. 2.8, it is straightforward to estimate $\mathbf{B}(\mathbf{r})$ from Eq. 2.7 and thus solve the forward problem. By making some assumptions about the volume conducting properties of the head and about the current distribution, V can be solved either numerically or even analytically in some cases.

2.4.2 Current dipole

For solving V in Eq. 2.8, one needs a model for primary current density. A commonly used approach is to model current density as a superposition of current dipoles. A dipole is a mathematical construct, a point-like source of an electric field defined by its location $\mathbf{r_Q}$ and moment $\mathbf{Q}$. The primary current by a single dipole can then be expressed using Dirac's delta function $\delta(\mathbf{r})$:

$$\mathbf{J_p}(\mathbf{r}) = \mathbf{Q}\delta(\mathbf{r} - \mathbf{r_Q}). \tag{2.9}$$

A current dipole also reflects our knowledge of neuronal currents. As shown in section 2.1.3, the field generated by the PSP that generates most of the measurable signal is fairly dipolar in nature when viewed from a distance. It is worth noting that here a current dipole denotes, conceptually, a patch of cortex with synchronously active pyramidal cells.

2.4.3 Volume conductor models

A typical volume conductor model for the head is a sphere. As the shape of the head and the brain is fairly spherical, this simple approximation is a useful tool for MEG/EEG. With the spherical conductor model, the solution for the forward problem (Eq. 2.7) can be solved based on the radial component of the magnetic field:

$$\mathbf{B_r}(\mathbf{r}) = \frac{\mu_0}{4\pi} \int \mathbf{J_p}(\mathbf{r}') \times \frac{\mathbf{r} - \mathbf{r}'}{\mid \mathbf{r} - \mathbf{r}' \mid^3} \cdot \mathbf{e_r} dv', \tag{2.10}$$

where $\mathbf{e_r}$ is a unit vector radial to the sphere surface (Sarvas 1987). Note that with this derivation of $\mathbf{B_r}(\mathbf{r})$, the magnetic field outside the head could be estimated without any information about the volume currents. However, other components of $\mathbf{B_r}$ are affected by the volume currents.

A more realistic model for the conductivity profile of the brain can be acquired by using, for example, a boundary element model (BEM, Hämäläinen and Sarvas 1989). In practice, when estimating the location of an isolated current dipole, the simple spherical model has an accuracy of 2-4 mm, which can be improved only marginally with the use of more realistic head geometries (Leahy et al. 1998; Crouzeix et al. 1999; Tarkiainen et al. 2003). These more complex conductivity models are of use mainly when focusing on activity in anterior frontal and deep brain regions.

When considering the special case of a dipolar source in a spherical conductor, the magnetic field outside the sphere assumes an analytical form (Sarvas 1987):

$$\mathbf{B}(\mathbf{r}) = \frac{\mu_0}{4\pi F^2}(F\mathbf{Q} \times \mathbf{r_Q} - (\mathbf{Q} \times \mathbf{r_Q} \cdot \mathbf{r})\nabla F), \tag{2.11}$$

where $F = a(ra + r^2 - \mathbf{r_Q} \cdot \mathbf{r})$, $\nabla F = (r^{-1}a^2 + a^{-1}\mathbf{a} \cdot \mathbf{r} + 2a + 2r)\mathbf{r} - (a + 2r + a^{-1}\mathbf{a} \cdot \mathbf{r})\mathbf{r_Q}$ and $\mathbf{a} = \mathbf{r} - \mathbf{r_Q}$. From Eq. 2.11 it also follows that radially oriented sources do not produce any magnetic field outside the sphere. In the case of MEG, this means that in the gyri, where pyramidal cells are roughly radially oriented, the measured signal would be diminished. However, it has been shown that only a very small part of gyri is invisible to MEG (Hillebrand and Barnes 2002).

2.4.4 Inverse problem solution

With models for the current distribution and the shape of the volume conductor, we can estimate the solution for the inverse problem. When using

equivalent current dipole as a model for current distribution, the source that best fits the measured data is called an equivalent current dipole (ECD). At a given time instant, the parameters of an ECD (location, orientation and amplitude) can be estimated from the MEG measurement with a least-square search. Usually a subset of MEG sensors is used in order to better constrain the search space. This search also gives a confidence interval for the ECD location parameter. If several brain regions need to be included in the model, a multi-dipole model is constructed by fitting more ECDs individually at different time instances or with a different set of sensors. The validity of an ECD may be estimated with the goodness-of-fit value:

$$g = \frac{1 - |b - \hat{b}|^2}{|b|^2}, \tag{2.12}$$

where b is the measured signal and $\hat{b}$ is the estimated signal (obtained via the forward solution). The temporal behavior of these sources can be determined by fixing the ECD location and orientation parameters and allowing the amplitude to vary to explain as much of the data as possible.

Brain activity can also be modeled with a mapping approach: instead of estimating parameters for one source area at a time, one may try to explain the measured signal with a large number of spatially fixed dipoles. The sources can be confined to the cortical sheet. This type of approach is called distributed source modeling. Because in these approaches the number of estimated parameters outnumbers the measurements, the inverse problem solution is underdetermined. A unique solution can be, however, achieved by imposing additional constraints on the data. Typically these types of methods seek to explain the data using a source distribution with the smallest norm. If this norm is of type L2 (sum of squared amplitudes, i.e., minimum overall power), the method is referred to as Minimum Norm Estimate (MNE, Hämäläinen and Ilmoniemi 1994), whereas methods using type L1 norm (sum of absolute amplitudes, i.e., minimum overall current) are called Minimum Current Estimates (MCE, Matsuura and Okabe 1995; Uutela et al. 1999).

2.4.5 Beamforming

An alternative to ECD or distributed source modeling is a type of localization technique called beamforming. Beamforming aims to determine the activation time course at a given location independently of the other brain

regions. This is done with a spatial filter which seeks to maximize gain from one region while suppressing input from the others. A spatial filter is essentially a set of weights that define a weighted sum of the sensor-level MEG signal. Mathematically this equals

$$\mathbf{y} = \mathbf{W}^T\mathbf{x}, \tag{2.13}$$

where y is the time course of activity at a given location, **W** is the weight matrix of the spatial filter and x is the measured signal. A map of activity is then obtained by moving the spatial filter across the cortex and finding a different set of weights for each location. By applying principles of linearly constrained minimum filtering (LCMV, Van Veen et al. 1997) to MEG/EEG data, it can be shown that the best least square fit for the weights **W** at location r can be determined as follows:

$$\mathbf{W} = \frac{\mathbf{C}^{-1}\mathbf{L}}{\mathbf{L}^T\mathbf{C}^{-1}\mathbf{L}}, \tag{2.14}$$

where **C** is the cross-covariance matrix of the measured data and **L** is the forward solution for a source at location r (Gross and Ioannides 1999). The approach seeks to minimize the interference of other sources and constrain the gain from r to a unit response. This type of beamforming is sometimes referred to as adaptive beamforming, because the covariance **C** makes the estimate dependent of the data itself. Beamforming was initially developed for radar and sonar use (Van Veen and Buckley 1988), but has since been applied successfully to analysis of cortical rhythmic activity measured with MEG/EEG (e.g. Robinson and Vrba 1999; Gross et al. 2001). However, using beamformers for analysis of evoked responses is problematic due to an insufficient covariance estimate: a number of time samples that exceeds the number of channels by a factor of 3-4 is needed for a good covariance estimate (Van Veen et al. 1997). As evoked responses have a short duration, this criterion is difficult to meet.

LCMV beamformers have been shown to converge to minimum norm solutions with an *a priori* assumption of uncorrelated sources (Mosher et al. 2003). The beamforming approach does not require any assumptions about the number of sources and can be performed for a limited volume at a time. A major theoretical weakness of beamforming is that it is blind to perfectly correlated sources. In practice, however, sources with quite high correlation can be modeled successfully with LCVM beamformers (Van Veen et al. 1997; Sekihara et al. 2002).

2.4.6 Analysis of rhythmic activity

Rhythmic activity is rarely phase-locked to a stimulus or task. Thus, averaged evoked responses will not capture this type of brain activity as averaging removes non-phase-locked responses. To identify the types of oscillatory activity included in the data, one typically starts the data analysis by examining the spectra of the measured signal at the MEG sensor level. With the Welch's method (Welch 1967), the spectrum is estimated from fast Fourier transforms (FFT) of short, partially overlapping data segments and averaged over all segments.

The task or stimulus-related time course of signal strength in a certain frequency band can be quantified by band-pass filtering the signal to the desired frequency range, rectifying and averaging over trials (TSE, Temporal Spectral Evolution, Salmelin and Hari 1994b). Another technique for sensor-level evaluation of rhythmic activity is Time-Frequency Representation (TFR, Tallon-Baudry et al. 1997). It shows the evolution of MEG signal as a function of time and frequency similarly to, e.g., spectrograms for sound signals in sound processing.

Cortical sources of rhythmic activity may be estimated with sequential ECD modeling (Salmelin and Hämäläinen 1995). In this approach, a normal dipole fitting scheme is applied to several batches of raw data filtered to desired frequency band, with dipoles fitted at small time intervals (e.g. every 10 ms). Because the SNR of raw data is far below that of an averaged evoked response, one needs to collect large amounts of dipoles that form reliably identifiable clusters. The number of dipoles in the clusters is reduced by requiring them to explain the data as well as possible, i.e. setting acceptance thresholds for goodness-of-fit and confidence interval values. The final selected source model is the ECD that best accounts for the observed task/stimulus related modulations. The time evolution of the source can be estimated with a TSE curve similar to estimations at the sensor level. Sequential dipole fitting was used successfully in Publication I.

Lately, minimum norm methods and beamforming have been applied to the analysis of rhythmic activity. Beamforming can be transformed into the frequency domain by substituting the cross-covariance in Eq. 2.14 with cross-spectral density (Gross et al. 2001) or by estimating the covari-

ance from broad-band MEG signals and then passing the narrow-band signal through the spatial filter (synthetic aperture magnetometry, SAM, Robinson and Vrba 1999; Barnes et al. 2003). For an overview on beamforming with MEG, see the review by Hillebrand et al. (2005). In this Thesis, the cross-spectral density approach was used in a method called Dynamic Imaging of Coherent Sources (DICS). It will be discussed in detail in section 2.6.

2.5 Functional connectivity

Exploration of the brain function based on separate active areas and their time courses of activation has been successful, but in recent years the focus has been shifting towards the way these areas operate in synchrony. Interactions between areas may reveal important functional properties of the neuronal system and it has even been claimed to be vital for cognition (Singer 1999; Varela et al. 2001). Connectivity has been explored in several studies on animals and humans (e.g. Büchel and Friston 1997; Logothetis 2003; Mechelli et al. 2004; Penny et al. 2004) using functional magnetic resonance imaging (fMRI). However, the slow hemodynamic response limits the time scales that can be accessed with fMRI measurements. As behaviorally relevant brain synchronization is likely to happen at a high temporal rate across the cortex, MEG, with its millisecond time resolution, should be well suited for addressing such phenomena. Indeed, synchronization of oscillatory cortical activity has been proposed as a prime candidate mechanism for connecting different cortical areas (Singer and Gray 1995; Varela et al. 2001).

When observing two cortical areas and their time series of activation, several methods exist for quantifying their interaction. Focusing on the methods in the frequency domain, the most common measure of dependency between signals is coherence. It is defined via power spectral densities as

$$\mathbf{Coh} = \frac{|\mathbf{P_{xy}}|^2}{\mathbf{P_{xx}}\mathbf{P_{yy}}}, \tag{2.15}$$

where $\mathbf{P_{xx}}$ and $\mathbf{P_{yy}}$ refer to power spectral densities of signals $\mathbf{x}$ and $\mathbf{y}$, and $\mathbf{P_{xy}}$ is the cross-spectral density of the two signals. Coherence takes values between 0 and 1, with $\mathbf{Coh} = 1$ indicating complete synchrony. In practical data analysis, it can be robustly implemented, is fast to compute,

and has been widely used in EEG to estimate interactions between different brain regions (Nunez et al. 1997). Coherence is used in this Thesis as the primary measure of connectivity (Publication V).

It is important to be aware of the limitations of coherence measures. First, this approach cannot distinguish between a case where areas A and B are connected directly from a case where A and B are connected via an area C. A method called partial coherence (Dahlhaus et al. 1997) has been developed to help distinguish between these two cases. Second, coherence is influenced by both the amplitude and phase of the signal. Thus, even in a case of total phase synchrony, coherence might yield relatively low estimates of connectivity. Since the phase information of the signal may play an important role in cortical connectivity (Singer and Gray 1995; Lachaux et al. 1999; Varela et al. 2001), methods relying only on the phase synchrony are also used. The most common of these measures are called phase-locking value (PLV, Lachaux et al. 1999) and synchronization index (SI, Tass et al. 1998). PLV is defined as

$$PLV(t) = \frac{1}{N}|\sum_{n=1}^{N} e^{i\theta(t,n)}|, \tag{2.16}$$

where $\theta(t,n)$ is the instantaneous phase difference between two signals at time t and trial n. PLV can further be tested for statistical significance with the use of surrogate data. SI is based on the notion of $n:m$ phase-locking value defined as

$$\varphi_{n,m}(t) = n\phi_1(t) - m\phi_2(t), \tag{2.17}$$

where t is time, n and m are integers and $\phi_{1,2}$ the normalized phases of two signals obtained via Hilbert transform. The preferred phase difference between two signals is then acquired from cyclic relative phase defined as the modulus of Eq. 2.17. SI is computed from the distribution of the cyclic phase either based on Shannon entropy or conditional probability (Tass et al. 1998).

Methods have further been developed to estimate whether the link between two areas has a primary direction of information flow or whether the information flow is bidirectional. Granger causality (Granger 1980) and partial directed coherence (Sameshima and Baccala 1999) are based on autoregressive modeling, i.e., they seek to predict one signal on the basis of another. Directionality index (Rosenblum and Pikovsky 2001) is based on the instantaneous phases of the signals and is the continuation

of the phase synchrony line of analysis. In Publication V, partial Granger causality (Geweke 1982; Guo et al. 2008) was used as a measure of directionality of information flow. It has superior performance over regular Granger causality in the presence of hidden or latent variables, which is a very possible problem in the case of EEG/MEG recordings.

2.6 Dynamic Imaging of Coherent Sources

Dynamic Imaging of Coherent Sources (Gross et al. 2001) is a versatile tool for mapping power distribution and connectivity on the cortex. It utilizes the principles of adaptive beamforming (see section 2.4.5) by building a spatial filter which employs the cross-spectral density (CSD) matrix as the representation of dependencies of oscillatory components in the MEG signal.

As mentioned in section 2.4.5, beamforming is based on the concept of cross-correlation between signals. For signals $\mathbf{x}$ and $\mathbf{y}$, it is defined under wide-sense stationary assumption as

$$\varphi_{\mathbf{x},\mathbf{y}}[l] = E\{\mathbf{x}[n]\mathbf{y}^T[n+l]\}, \tag{2.18}$$

where E is the expectation value and l is the time lag. The CSD is then defined as the Fourier transform (FT) of $\varphi_{\mathbf{x},\mathbf{y}}$:

$$\mathbf{C}(f) = FT\{\varphi_{\mathbf{x},\mathbf{y}}[n]\}_f = \sum_{n=-\infty}^{\infty} \varphi_{\mathbf{x},\mathbf{y}}[n]e^{-i2\pi fn}, \tag{2.19}$$

where $\mathbf{C}$ is the cross-spectral density. This can be directly calculated by using Fourier transforms ($\mathbf{X}$, $\mathbf{Y}$) of signals $\mathbf{x}$ and $\mathbf{y}$:

$$\mathbf{C}(f) = \mathbf{X}(f)\mathbf{Y}(f). \tag{2.20}$$

In practice, the estimation of CSD from data is typically done with Welch's method. Instead of a Fourier transform one can use wavelets which scale their time resolution with frequency. This latter approach is used in event-related DICS (erDICS, Publication II).

The CSD matrix is constructed by repeating the estimation of $\mathbf{P}_{\mathbf{xy}}$ for all MEG sensor pairs. Additionally, external signals such as EOG or EMG can be included into the CSD matrix estimation. The diagonal of the resulting matrix will store the power spectral densities. Sensor-level coherence can be directly accessed with the matrix by using Eq. 2.15.

A spatial filter is constructed in order to achieve cortical-level power and coherence mapping. In DICS, the spatial filter is defined slightly differently than in the theoretical beamformer explained in section 2.4.5. Mainly, a regularization parameter is included in the minimization problem, which reads as follows (Gross and Ioannides 1999):

$$min[E\|\mathbf{AX}\|^2 + \alpha\|\mathbf{A}\|^2], \text{ subject to } \mathbf{AL(r)} = \mathbf{I}, \tag{2.21}$$

where **A** is the spatial filter transformation matrix, **X** is the Fourier transformed data from all sensors and **L(r)** contains the solutions of the forward problem at **r** for two tangential orthogonal dipoles. α is the regularization parameter, which controls the spatial extent of the spatial filter. The matrix **A** is solved by forming the Lagrange function for Eq. 2.21 and finding its minimum. The result is

$$\mathbf{A(r}, f) = (\mathbf{L}^T(r)\mathbf{C_r}(f)^{-1}\mathbf{L(r)})^{-1}\mathbf{L}^T\mathbf{(r)C_r}(f)^{-1}, \tag{2.22}$$

where $\mathbf{C_r}(f) = \mathbf{C}(f) + \alpha\mathbf{I}$. The CSD estimate between four source combinations at locations $\mathbf{r_1}$ and $\mathbf{r_2}$ is

$$\mathbf{C_s}(\mathbf{r_1}, \mathbf{r_2}, f) = \mathbf{A}(\mathbf{r_1}, f)\mathbf{C}(f)\mathbf{A}(\mathbf{r_2}, f). \tag{2.23}$$

By substituting $\mathbf{r_1} = \mathbf{r_2}$, one gets the power estimation at a given location:

$$\mathbf{P}(\mathbf{r}, f) = \mathbf{C_s}(\mathbf{r}, \mathbf{r}, f) = \mathbf{A}(\mathbf{r}, f)\mathbf{C}(f)\mathbf{A}(\mathbf{r}, f). \tag{2.24}$$

The CSD matrix can be investigated via its singular values. If one is far larger than the other, the cross spectrum can be attributed to a single source with a fixed orientation determined by the eigenvectors, and CSD can be determined with the larger singular value:

$$\mathbf{c_s}(\mathbf{r_1}, \mathbf{r_2}, f) = \lambda_1\{\mathbf{C_s}(\mathbf{r_1}, \mathbf{r_2}, f)\} \tag{2.25}$$

where $\lambda_1\{\}$ denotes the largest singular value. Similarly for power:

$$p(\mathbf{r}, f) = \lambda_1\{\mathbf{P}(\mathbf{r}, f)\} \tag{2.26}$$

With Eq. 2.25 - 2.26, coherence at cortical location **r** can be expressed as

$$Coh(\mathbf{r_1}, \mathbf{r_2}, f) = \frac{|\mathbf{c_s}(\mathbf{r_1}, \mathbf{r_2}, f)|^2}{p(\mathbf{r_1}, f)p(\mathbf{r_2}, f)} \tag{2.27}$$

For mapping cortical power or coherence, the approach illustrated above is applied on a grid spanning the brain. Typically, the grid point distance

is 5-10 mm, and the deep structures are removed from the grid, as MEG is not very accurate there (Tarkiainen et al. 2003). Hence, the coherence estimate from these areas may lead to spurious connection estimates as several sites might see the same activity. Power maps are noise normalized either to white noise or to estimation of an empty measurement room noise. Coherence maps need a reference point, which is either an external signal or a brain region. It is possible to map coherence between all possible source area combinations and to infer from there a map of functional connectivity.

3. Aims of the Thesis

The goal of the Thesis was to better understand the rhythmic brain activity as a marker of complex brain processing. The specific research goals were to

- investigate what power level modulations can tell about brain processing in language-related motor tasks. The 20-Hz rhythm was used as an index of motor cortex activation (Publication I).

- create a method for event-related mapping of power level modulation of rhythmic activity by expanding cross-correlation estimation in DICS using wavelets (Publication II).

- compare task effects in complex cognitive processing as conveyed by modulation of rhythmic activity and the far more commonly used evoked responses. Here, a picture naming experimental paradigm was used to expand the search beyond primary sensory areas (Publications III and IV).

- expand event-related power mapping further to time-sensitive mapping of functional connectivity. Connectivity was mapped during a priming experiment (Publication V).

4. Summary of studies

4.1 Indexing mouth-movement-related activity via brain oscillations (PI)

Mouth movements are essential in various human actions, from eating and chewing to expressing emotions and speaking. In the cortex, the most important functional area for controlling mouth movements is the face representation area of the primary motor cortex (M1) (Penfield and Boldrey 1937; Huang et al. 1989), which is part of the sensorimotor cortex (SMC) along the central sulcus. This area is involved in the control of the lip, tongue and jaw movements.

Besides motor movement control, M1 seems to also be a part of the brain network dealing with visuomotor mapping (e.g. mapping letter symbols to corresponding motor actions). Visuomotor mapping has been demonstrated in monkeys, when they map colors into arm movements (Zhang et al. 1997). In humans, preparatory activity in the face area of M1 before articulation has been shown with MEG recordings in an overt reading task (Salmelin et al. 2000). Activation is not observed in the hand representation areas (evidence from MEG: Salmelin et al. 2000; Salmelin and Sams 2002). However, the M1 activity seems to coincide more with movement execution than with preparation. Interestingly, the hand M1 involvement seems to differentiate between speech and nonspeech mouth movements.

In Publication I, we used movement-related changes of the 20-Hz range rhythm as an index of motor cortex activation (Hari and Salmelin 1997; Pfurtscheller and Lopes da Silva 1999) to investigate how a varying de-

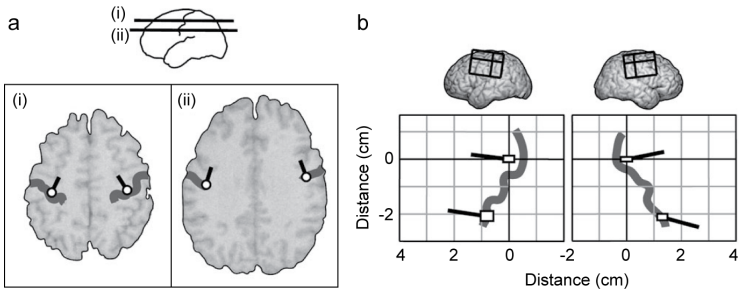

Figure 4.1. (a) The mean location (dot) and orientations (tail) of ECDs shown on two axial planes (i and ii). (b) The mean location and orientation of ECDs on left and right lateral views. Central sulcus is plotted with the thick dark line. Adapted from PI.

gree of speech-likeness of simple and complex mouth movements is reflected in the rhythmic brain activity in the mouth and face motor areas. Besides serving as a highly specific marker of M1 involvement, the 20-Hz rhythm is a valuable measure also because is not markedly disturbed by electric and magnetic fields originating from facial muscles (Salmelin et al. 2000; Salmelin and Sams 2002). The difference between the suppression minimum and the post-movement rebound maximum was selected as the measure of task-related activation in M1. This measure was further normalized by the level of activity at rest.

The experimental tasks were simple one-item mouth movements based on phonemes or gestures and complex four-item movements that ranged from non-speech gestures to real words in four steps: the stimuli were either a string of gestures, consonant strings, CVCV (Consonant, Vowel) pseudowords or words (See Figure 1 in PI). The subjects were instructed to perform the mouth movements silently.

The cortical source areas were modeled with sequential ECDs (see section 2.4.6 for details) from three 30-s blocks of the non-averaged MEG data set. The ECD analysis was conducted on subsets of 20-28 sensors covering the maximum sensor-level TSE modulation, separately for each hemisphere. An ECD model of sources bilaterally in the M1 hand and face areas was constructed for each individual. For comparison and visualization, the ECD locations were transformed into a standard brain (Schormann et al. 1996; Woods et al. 1998a; Woods et al. 1998b) using elastic transformation (Roland and Zilles 1996). The mean locations of the source areas are shown in Figure 4.1 and their time courses of activation in Figure 4.2.

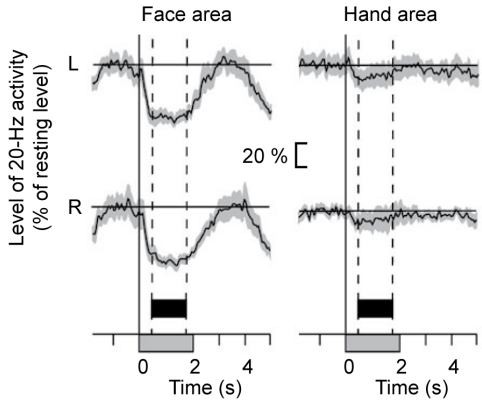

Figure 4.2. Time courses of 20-Hz modulation in the face and hand areas for word stimuli. The black rectangles indicate the mean movement durations and the gray rectangles the duration of stimulus presentation. Adapted from PI.

These data suggested that the face motor cortex not only controls the muscle activity during speech but is also involved in coordination of visuomotor mapping and/or movement sequencing. In the face areas, we found that the onset and offset of suppression of the 20-Hz activity was earlier in the left than the right hemisphere, both for speech and non-speech movements. In the hand areas, the modulation of 20-Hz activity was systematically stronger for non-speech than speech-related mouth movements. This finding may reflect either more focal M1 activation specifically for language or importance of both mouth and hand coordination in non-speech mouth movements.

From a data analysis point of view and for the purpose of this Thesis, PI illustrated typical properties of oscillatory brain signals: duration in order of seconds and the suppression – rebound pattern seen in 20-Hz rhythms. It also became obvious that while in this study the 20-Hz rhythm was easy to localize and the results showed functionally relevant modulation, a more accommodating approach was needed for less restricted mapping of cortical rhythms. Special care should be taken when modeling suppressions, because the decreased SNR makes them difficult to model directly. To this end, we turned to beamforming in study PII.

4.2 A method for spatiotemporal mapping of rhythmic activity: erDICS (PII)

Since DICS was originally designed to be used with continuous tasks, a more flexible version was needed for time-sensitive analysis of rhythmic modulations in an event-related experimental paradigm. If applied directly, DICS cannot, e.g., discover all the details of the modulatory behavior of brain oscillations seen in study PI. The main motivation of study PII was therefore to expand the use of DICS into a more refined time-scale by exploiting a wavelet-based filter bank technique. With this approach, it is possible to identify increases and decreases of rhythmic activity by comparing different time points (e.g. baseline vs. activation). This is especially vital for mapping decreases of rhythmic activity, which cannot be easily examined due to decreased SNR during suppression. A statistical testing procedure was also introduced in study PII. This new method was tested on simulated and real MEG data sets. In this study, erDICS was used only for power mapping. Later, in study PV, it was further exploited for connectivity estimation.

DICS can be expanded as an event-related method by estimating the CSD matrix as a function of time. Power and coherence mapping can then be performed in the usual manner (see section 2.6), but as a function of time. A short-term FFT could have been applied as well, but it suffers from the rigid time resolution inherent in Fourier transform estimation: roughly 1 s of data would be needed for proper estimation of spectral properties. Wavelets, however, scale their time resolution with frequency, allowing for mapping of fast changes in high frequency spectral power, at the cost of frequency resolution.

In PII, the CSD matrix was estimated with the use of a Morlet wavelet filter bank. A Morlet wavelet (Morlet et al. 1982) is a sinusoidal signal modulated with a Gaussian envelope (modified from Tallon-Baudry et al. 1997):

$$M(t, f_c, \sigma_t) = Se^{-t^2/(2\sigma_t)}e^{i2\pi f_c t}, \tag{4.1}$$

where t is time, f_c is the center frequency of the wavelet and σ_t is the standard deviation of the wavelet in the time domain. The scaling parameter S ($(\sigma_t\sqrt(\pi))^{1/2}$) normalizes the energy of the wavelet to 1. The standard

deviation of the wavelet in the frequency domain is

$$\sigma_f = 1/(2\pi\sigma_t). \tag{4.2}$$

The ratio $w = f_c/\sigma_f$ is called the width of the wavelet and sets the relationship between time and frequency resolution. Full width at half maximum (FWHM) of the wavelet in the time and frequency domains (w_t and w_f, respectively) quantify the resolution of the wavelet:

$$w_t = \sqrt{2 * ln(2)}\,/\pi * w/f_c, \tag{4.3}$$

$$w_f = 2\sqrt{2 * ln(2)} * f_c/w. \tag{4.4}$$

As can be noted from Eq. 4.3 - 4.4, the temporal resolution is improved with smaller w and higher central frequency.

By estimating a time-dependent CSD matrix ($\mathbf{C_r}(f,t)$) with the wavelet approach, Eq. 2.22 now reads:

$$\mathbf{A}(\mathbf{r},f,t) = (\mathbf{L}^T(\mathbf{r})\mathbf{C_r}(f,t)^{-1}\mathbf{L}(\mathbf{r}))^{-1}\mathbf{L}^T(\mathbf{r})\mathbf{C_r}(f,t)^{-1}. \tag{4.5}$$

We applied two approaches for the estimation of the CSD matrix: (i) Single-trial CSDs, where CSDs and power maps are evaluated for each trial separately, and (ii) a mean CSD approach where the CSD is averaged over all trials. We evaluated the feasibility of these approaches with simulated MEG data, where three artificial oscillatory sources had an initial suppression of activity followed by an increase of the power level.

The results of the power mapping for (i) and (ii) are shown in Figure 4.3 for data with an SNR of 1/5. In the case where the suppression and increase of activity were separated by 0.3 s (Figure 4.3a), the mean CSD approach yielded accurate localization and timing, whereas for the single-trial CSD approach the active areas were more spread out temporally and spatially. This was mainly due to the poor SNR of the single-trial CSD and the limited time resolution of the wavelet, which caused temporally close suppressions and increases to overlap. When the time separation between the events was increased to 1.2 s (Figure 4.3b), the different types of activations could be separated with the single-trial CSD approach, but the mean CSD approach still outperformed it. Therefore, the mean CSD approach was chosen as the preferred approach.

For the mean CSD approach, the spatial filter was applied to the raw data to extract the time series of the active areas. The data was then further

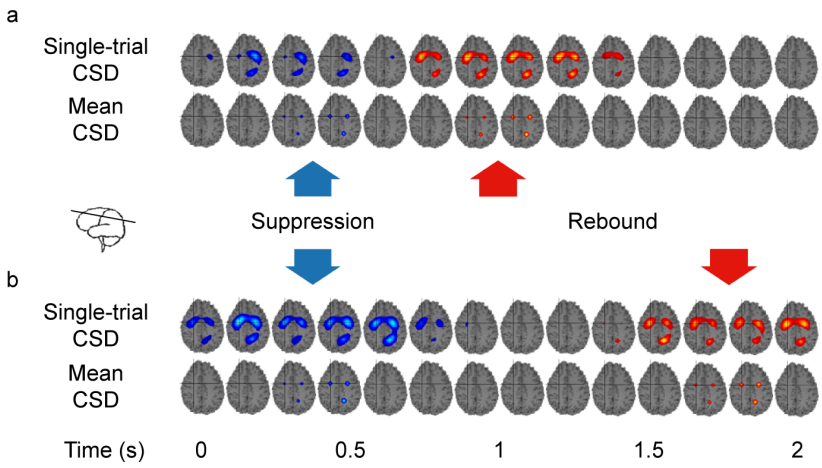

Figure 4.3. Comparison of the mean CSD and single-trial CSD approaches with simulated data. The delay between suppression and increase of activity was 0.3 s in (a) and 1.2 s in (b). Adapted from PII.

band-pass filtered to the selected frequency band and instantaneous amplitudes were estimated with the absolute values of the Hilbert transform. The statistical significance of the power change between two conditions (here, "baseline" and "active" time intervals) was estimated with a random permutation test (Nichols and Holmes 2002) based on trial-to-trial power level distributions. The random permutation test is a nonparametric test that requires minimal assumptions about the data. The main demand is that the conditions are interchangeable (Holmes et al. 1996).

The voxel-level random permutation test was implemented by first estimating a statistic between "baseline" and "active" conditions. We used the common Student's *t*-test for this purpose. In the second step, the samples in the two distributions were randomly shuffled and a new t-value was estimated. This step was then repeated 5000 times and the new t-values were collected into a new test distribution. The p-value of the permutation test was then acquired by comparing the original t-value to the test distribution. Because the test is performed in all of the voxels, the level of false positives has to be controlled. This was achieved via a maximum-statistics approach. The maximum and minimum t-values were collected from all of the voxels into new maximum/minimum distributions. The final p-values were estimated by comparing the original t-value to the maximum/minimum distributions.

The performance of the "mean CSD" approach and statistical testing was evaluated with simulated data under varying SNRs. For this purpose, we

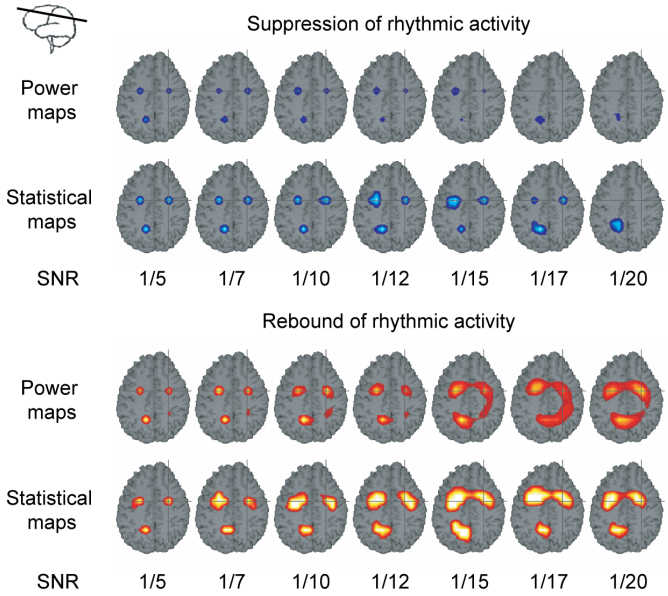

Figure 4.4. Effects of SNR on erDICS power and statistical maps for simulated data. Adapted from PII.

also included a fourth source in the simulation. This source acted as a "fake" source, producing a strong burst (20 times larger than the other three sources) in 1/20 of the trials. All sources were correctly identified down to an SNR of 1/15 (Figure 4.4). Increases of rhythmic activity could be identified even at the SNR level of 1/20. The "fake" source was preserved in the power maps, but was eliminated by the random permutation test.

The erDICS was applied to two sets of real MEG data. The first set was from an index finger lifting task (from study PI) and the second set was from a study where the subjects were instructed to silently read words presented at 3 s intervals (Wydell et al. 2003). For the first data set, erDICS showed a clear contralateral activation of the motor cortex of the 20-Hz rhythm, as expected (Figure 4.5a). In the cognitively more demanding task of word reading, erDICS identified four active areas (Figure 4.5b). The validity of these identified source areas was good, as the multi-ECD model constructed with them explained over 70% of the variance of the data over the whole analysis time window for both data sets.

In conclusion, study PII showed that erDICS can readily be used for mapping event-related induced rhythmic brain activity in individual subjects. In PIII, erDICS is used to map brain areas of rhythmic activity. Here,

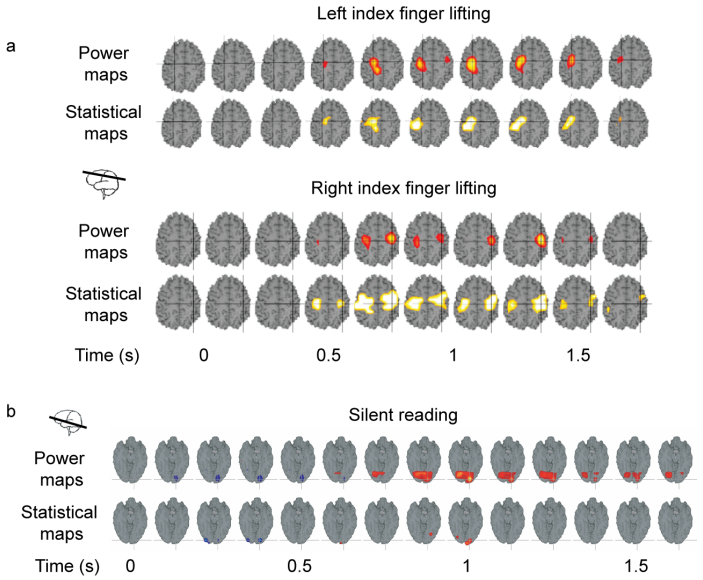

Figure 4.5. erDICS power and statistical maps for (a) an index finger lifting task (20-Hz) and (b) silent reading task (10-Hz). Adapted from PII.

and in PIV, the studies focused on the mapping of power modulation. The erDICS can, however, also be applied for the original purpose of DICS: studying functional connectivity. This important functionality was later implemented in study PV.

4.3 Rhythmic activity and evoked responses in a picture naming task (PIII and PIV)

The relationship between evoked responses and spontaneous rhythmic brain activity has been under debate. In the so-called additive model, the two phenomena are considered separate, with the evoked responses independent of the ongoing spontaneous oscillations (Shah et al. 2004; Mäkinen et al. 2005; Mazaheri and Jensen 2006). However, phase-resetting of brain rhythms has been shown as a possible generator of evoked responses in a few cases (Makeig et al. 2002; Penny et al. 2002). Also, slow evoked responses have been hypothesized to emerge from asymmetry of rhythmic amplitudes, i.e., the rhythmic activity would not have a zero mean, but rather the peaks would be modulated more than the troughs (Nikulin et al. 2007; Mazaheri and Jensen 2008).

When focusing on low-level sensory processing, studies addressing evoked

responses and rhythmic activity with similar experimental designs found activity largely in the same brain areas in the occipital cortex and around the parieto-occipital sulcus (visual processing), as well as along the central sulcus (somatosensory areas) (Karhu et al. 1991; Vanni et al. 1996; Hari and Salmelin 1997; Vanni et al. 1997). However, when the sources of evoked responses and rhythmic activity were analyzed from the same data set, the task-specific functionality and hemispheric balance differed (e.g. Schnitzler et al. 1997; Salmelin et al. 2000). Direct comparisons between the two measures of activity have not been extensively made outside the primary sensory areas and most of the MEG and EEG studies have focused on only either evoked responses or rhythmic brain activity.

Study PIII introduces a picture naming study that relies on the analysis of evoked responses. Study PIV uses this data set together with two other data sets from picture naming tasks (Vihla et al. 2006; Liljeström et al. 2009) to evaluate the relationship between evoked responses and rhythmic activity.

4.3.1 Picture naming task

A picture naming task is widely used behaviorally for assessing the type of impairment in patients with brain damage (e.g. DeLeon et al. 2007; Mahon and Caramazza 2009) and in imaging studies for investigating word production, from visual analysis to accessing meaning and sound form to articulation. In evoked response studies, the sequence of cortical activity has been described to start with a transient occipital response less than 200 ms after the picture presentation. The activation has then been shown to proceed with more sustained responses to parietal and temporal areas after 200 ms and reaching frontal cortex after 300 ms (Salmelin et al. 1994; Indefrey and Levelt 2004; Vihla et al. 2006; Salmelin 2007; Hultén et al. 2009; Liljeström et al. 2009).

Study PIII used a picture naming paradigm for investigating vocabulary growth and maintenance of learned linguistic information in healthy subjects. The participants were shown black-and-white line drawings of tools that were either familiar (Fam, 50 pictures) or unfamiliar (100 pictures). The subjects then learned the name for half of the unfamiliar items (Name) while the rest remained unnamed (NoName). The subjects' brain activity was recorded with MEG after they had learned all of the

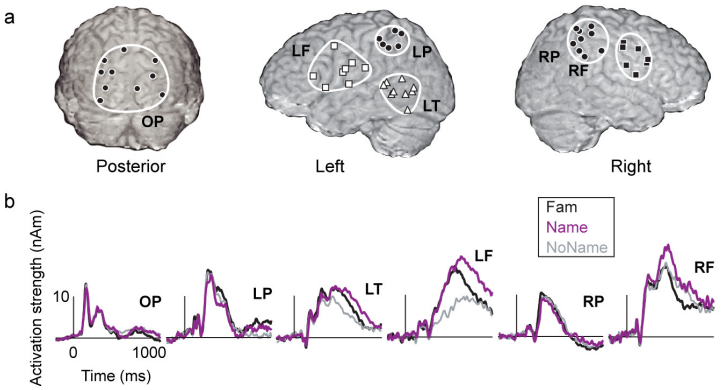

Figure 4.6. (a) Source areas of evoked responses for individual subjects, clustering in six brain regions (occipitoparietal (OP), left/right parietal (LP/RP), left temporal (LT) and left/right frontal (LF/RF)). (b) Mean time courses of activation across all measurements in the different brain areas. Adapted from PIII.

names. Afterwards, the maintenance of the learned information was evaluated with follow-up MEG measurements and behavioral tests 1 week, 4 weeks, 2 months and 10 months later. The evoked response source areas, across the six measurement days, were found in the same regions: the left temporal, the occipital and the bilateral parietal and frontal cortices. Although some subjects showed right temporal activation, it was not consistent enough across subjects to warrant group comparisons. The timing and activated areas were in line with earlier MEG studies (Figure 4.6).

Study PIII showed that the change in neural activation in the left temporal and parietal cortices over one week after learning predicted how much the activity to correctly named objects had changed by 10 months after learning (Figure 4.7).

4.3.2 Comparison between rhythmic activity and evoked responses

PIV sought to assess the relationship between evoked responses and brain rhythms. Three MEG data sets obtained from a picture naming paradigm were used for this purpose (PIII; Vihla et al. 2006; Liljeström et al. 2009) with altogether 31 data sets across the experiments. This type of experimental setup with high cognitive demands activates a large number of brain regions, thus enabling a thorough assessment of similarities between the two response types even beyond primary sensory brain areas. The source-level activity was analyzed separately by selecting the optimal

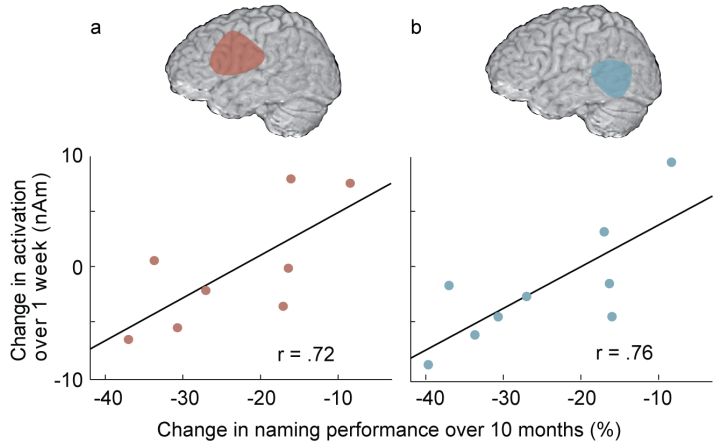

Figure 4.7. Change in activation from fully learned to 1 week after learning in the left frontal (a) and temporal (b) cortices correlated positively with the change in naming performance after 10 months. Adapted from PIII.

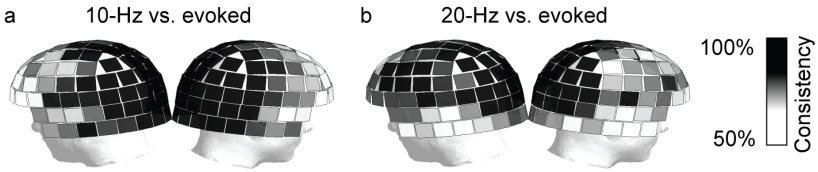

Figure 4.8. Consistency between evoked responses and modulation of 10-Hz (a) and 20-Hz (b) rhythmic activity at the sensor level. The overlap between the two measures was first evaluated for individual subjects and then merged across subjects and data sets. See PIV for details. Adapted from PIV.

methods best suited for each response type: evoked responses were previously analyzed in the original studies with ECD models and, for the study PIV, rhythmic activity was modeled using erDICS.

Analysis of rhythmic activity was performed using the frequency bands with the most salient task-related modulation of rhythmic activity: 7-12 and 17-22 Hz. Already at the sensor level (Figure 4.8), it was obvious that the spatial overlap between the measures was low. At the cortical level, rhythmic activity was most consistently localized in the visual and sensorimotor cortices, with some activity seen in the parietal and superior temporal areas (Figure 4.9).

For comparison of spatial overlap between the source locations of evoked responses and rhythmic activity, the brain was divided into 29 regions of interest in both hemispheres (Figure 4.9) with automated parcellation techniques (Fischl et al. 2004; Desikan et al. 2006) using the FreeSurfer software package (http://surfer.nmr.mgh.harvard.edu/). The correspon-

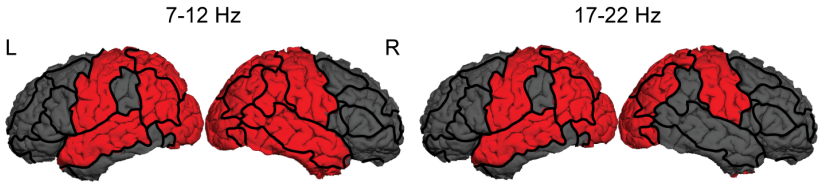

Figure 4.9. Source regions of rhythmic activity localized using erDICS. Red indicates brain regions in which modulation of rhythmic activity was identified in at least half of the subjects in any one of the three experiments. Adapted from PIV.

dence between the two measures was compared by estimating, for each source, the minimum distance to any source area of the other measure of activity. The sources were considered to be from the same brain region if the distance between them was less than 20 mm. This estimation was done separately for each subject. Two kinds of "hit rates" were estimated: (i) per brain region, with the rhythmic activity as the starting point, the ratio of subjects who had a source of evoked response in the same brain region with a rhythmic source, and (ii) per subject, with the evoked responses as the starting point, the percentage of sources of evoked responses with a source of rhythmic activity close-by (< 20 mm).

Across the three data sets, the per-region group-level convergence between evoked responses and rhythmic activity was most consistent in the lateral aspects of the right occipital cortex. Also, the medial occipital and the left pericentral cortex illustrated high convergence. In these areas, the time courses of the two measures were markedly different. In per-subject comparison, the hit rate between sources of evoked responses and rhythmic activity was on average 30%, exceeding 50% only for four out of 31 subjects. See Tables 1 and 2 in the original publication for details.

In brief, only weak spatiotemporal overlap was found between the evoked responses and rhythmic activity in the high-level cognitive task of picture naming. This suggests that the phase-locked evoked responses and modulation of rhythmic activity are largely detached phenomena and that both measures are needed for an accurate portrayal of brain activity.

4.4 Event-related functional connectivity during priming (PV)

The preceding studies (PI, PII and PIV) focused on the power modulations of rhythmic brain activity. erDICS can, however, also assess the

functional connectivity of brain regions via coherence measures, as described in section 2.6. In the study PV, erDICS was employed for tracking interactions between brain regions during a word priming experiment.

Priming refers to the phenomenon where exposure to a stimulus affects the processing of a subsequent stimulus. In language studies, this paradigm is commonly used to examine phonological and semantic processing. Typically, a subject is shown a word (prime), followed by another word (target) that has a related phonological or semantic content (Nobre and McCarthy 1994; Simos et al. 1997; Helenius et al. 1998). Behaviorally, priming leads to faster reaction times for a congruent target, while at the neural level priming leads to decreased neural activity. Faster processing is seen as a sign of increased efficiency of neural processing (Rossell et al. 2003), but the exact mechanism of how this happens remains unclear. PV investigated whether changes in functional connectivity might be involved in the increased efficiency during priming.

We hypothesised that priming would result in increased interareal synchronization (i.e., increased coherence between areas) for targets, in contrast to evoked responses where the level of activity decreases. Such a mechanism would suggest that the increased efficiency following priming would result from enhanced information transfer between brain regions, also manifesting as reduced processing demands in local neuronal assemblies. Connectivity analysis with erDICS was performed on an MEG data set, where subjects were shown lists of words that were related either semantically or phonologically. Results from the evoked response analysis (Vartiainen et al. 2009) indicated a strong priming effect in the bilateral middle superior temporal cortex (STC), in line with numerous other studies (Simos et al. 1997; Helenius et al. 1998; Marinkovic et al. 2003; Uusvuori et al. 2008). The left STC could be identified in all subjects via the evoked response analysis and, hence, connectivity was mapped between the left STC and all other brain regions in order to determine whether cortico-cortical interactions between brain areas were modified either by semantic or phonological priming. In addition, whether the main direction of information flow was to or from the STC was investigated.

In the experiment, subjects were shown a list of four words, one at a time, at 1-s intervals with a 2.1-s interval between word lists. The first three words were related either semantically or phonologically and the

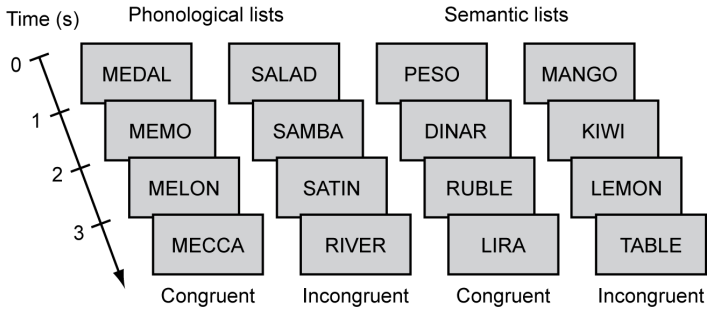

Figure 4.10. Experimental design, with examples of the word list types. Adapted from PV.

last word was either congruent or incongruent (Figure 4.10). Since our focus was on priming effects and not on differences between the processing of congruent/incongruent words, the analysis was done on the second and third words of the list.

The candidate time-frequency windows for priming effects in connectivity were identified at the sensor level. Time-dependent coherence was estimated with the same wavelet approach that was used in PII. The analysis focused on the time interval 250 to 650 ms after stimulus presentation where the priming effect had been detected in evoked responses (Vartiainen et al. 2009). The frequency analysis ranged from 5 to 25 and from 60 to 90 Hz. These frequency bands include the most salient modulations of rhythmic activity seen with MEG and avoided frequency bands easily contaminated by artifacts such as line noise. The reference sensor was the sensor closest to the left STC. Some sensors were discarded from the analysis as a cautionary step because power-level differences between two conditions can lead to spurious connectivity in coherence measures due to field spread (Schoffelen and Gross 2009). Therefore, if a sensor showed significant power differences between the second and third words of the word list in at least 3 neighboring time-frequency bins, it was discarded from the analysis. The final candidate time-frequency windows with significant coherence effects were identified with a cluster-based permutation test (Nichols and Holmes 2002; Maris and Oostenveld 2007).

Cortical-level connectivity analysis was performed with erDICS in the time-frequency windows identified at the sensor level. Coherence was estimated between the left STC and 1759 grid points covering most of the surface of the cortex at 6-mm intervals. Statistically significant connections were identified with permutation tests, across subjects. Paired

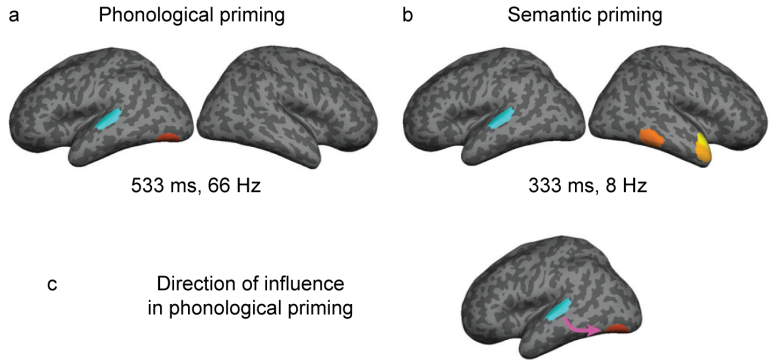

Figure 4.11. Brain regions with significantly increased coherence in (a) phonological and (b) semantic priming. (c) The significant direction of influence in phonological priming. Adapted from PV.

signed rank tests were used to assess possible confounding power differences between the second and third words for connections showing significant coherence effects.

The main direction of influence between the left STC and significantly connected brain regions was evaluated with partial Granger causality (Granger 1980; Geweke 1982; Guo et al. 2008). For directionality analysis, the time series of the STC and other brain regions were estimated with erDICS. A bootstrapping approach was implemented to evaluate whether the direction of influence measures exceeded statistical significance. If the lower limit of this confidence interval was above zero systematically across subjects (binomial test), the connection was considered to display a significant direction of influence at the group level; for the connections with significant directed components, the differences between the influence terms were tested with a one-sample *t*-test.

The connectivity analysis revealed priming effects as significantly increased coherence in one time-frequency window for each of the priming categories. For phonological priming, this window was centered at 533 ms and 66 Hz and for semantic priming at 333 ms and 8 Hz. In phonological priming, coherence increased between the left STC and the left occipital cortex (Figure 4.11a), whereas in semantic priming, coherence increased between the left STC and the right frontotemporal and inferior temporal cortex (Figure 4.11b). A main significant direction of influence was evident only in phonological priming, where the left STC was the driving node (Figure 4.11c).

The results of study PV indicate that corticocortical coherence increased during priming, thus supporting the notion of enhanced connectivity as a neural mechanism for increased efficiency during priming. Furthermore, phonological and semantic priming seemed to involve distinct brain connections with different directionality estimates, indicating a different role for the left STC in the two types of priming.

The event-related mapping of coherence with erDICS in study PV complements its power mapping capacity applied previously in study PIV. With both of these functionalities, erDICS is an excellent addition to a researcher's toolbox in the field of neuroscience.

5. Conclusions and discussion

This Thesis sought to better understand and model the ongoing rhythmic activity of the brain. The starting point was a study of motor cortex activity during a language related mouth movement task. Although not a new idea, this work showed that rhythmic activity does play a role in the visuomotor mapping network. However, from a data analysis point of view, it became clear that a more accommodating approach was needed for less restricted mapping of cortical rhythms. erDICS, a new event-related version of the DICS beamformer method was implemented to assist the modeling of rhythmic activity. The feasibility of this new method was shown with simulations and real MEG data.

Event-related DICS was applied to compare evoked responses and rhythmic activity in a high-level cognitive task of picture naming, with the conclusion that the two measures of cortical processes are largely detached and that both measures are needed for an accurate portrayal of brain activity. In this study, the rhythmic activity was mostly contained in the visual and sensorimotor cortices, with some activity seen in the parietal and superior temporal areas, whereas evoked responses could be modeled from several other areas as well.

Besides power level modulations, functional connectivity can also be mapped with erDICS. In PV, erDICS was used to investigate connections between the left STC and other cortical brain regions in a word priming study. Different brain networks were revealed for phonological and semantic priming. Furthermore, a directed link from the left STC to the left occipital cortex was revealed with partial Granger measures. As the statistical analysis applied to this data adhered to, by far, the most stringent methods currently promoted within the scientific community, there is a fair chance that some additional real effects might have been missed.

In future studies, to better assess the different connectivity patterns, one should either increase the number of subjects or apply statistical test less prone to false negative errors.

5.1 Beamforming – advantages and limitations

Beamforming has become a popular tool for mapping cortical rhythmic activity in MEG. It provides simultaneous mapping of multiple source areas and is a very versatile tool for investigating cortical rhythms that are not phase-locked to a stimulus or task. The resulting maps can also be subjected to statistical testing to find areas with stimulus or task-related modulation of rhythmic activity. While beamforming is not a solution to the inverse problem in a strict sense, as it is rather a scanning method, the processing of activation maps and identification of significantly active brain areas makes it at the very least a close relative of the inverse problem solution. Furthermore, since the spatial filter also provides time series for each investigated location, beamforming opens up possibilities for several analysis approaches requiring accurate temporal information. One such approach is the Granger causality measure used in this Thesis.

The main drawback of beamforming in general is that it cannot detect perfectly correlated sources. In MEG measurements of cortical rhythms, however, the brain signal itself is quite noisy and it is embedded in environmental noise, which reduces the SNR and, subsequently, coherence levels. Therefore, the problem of too perfectly correlated sources is minimal. The limitation should be kept in mind when creating simulated MEG data, since pure sinusoidal signals will be lost by beamforming and, therefore, extra caution must be taken to ensure low enough coherence levels by introducing enough noise and variability in the generated signals.

Modeling evoked responses is another major problem for beamformers. As mentioned in section 2.4.5, the sensor coverage of the 306-channel magnetometer actually works against mapping of evoked responses with beamformers, since the time samples required for a stable estimation of the covariance matrix increases with the number of channels. As evoked responses are fast transient events, with limited amount of data samples, it is difficult to map them with beamformers. This is unfortunate, because in PIV it would have been elegant to be able to model both evoked responses

and rhythmic activity with a beamformer and then find correlations at the cortical level by performing a statistical test for the activation maps. Measuring MEG signal at a faster sampling rate might help mapping evoked responses with beamformers.

5.2 Future topics

The basic properties of rhythmic activity in the brain remain elusive. In order to better understand them, it could be informative to look at the properties of the measured signal in a stochastic context. For example, asymmetry in the amplitude modulation of alpha rhythms has been shown to give rise to slow evoked responses (Nikulin et al. 2007; Mazaheri and Jensen 2008; van Dijk et al. 2010). More work is needed to see if this amplitude asymmetry exist in other types of rhythmic activity as well. An even more statistical viewpoint is the given by the reports of scaling law properties of the cortical rhythms (Linkenkaer-Hansen et al. 2001; Kello et al. 2010). Such systems are investigated in the context of phase transitions, where a small change near a critical point can propagate quickly throughout the system at several time scales. Some evidence suggest that abnormal changes in the scaling law properties of brain oscillations are linked with memory problems, such as in Alzheimer disease (Montez et al. 2009). When looking closely at the MEG signal, one can observe considerable intersubject variability in the cortical oscillations, implying that proper testing of different hypotheses will require a far larger number of subjects than are commonly used in MEG studies (10-15 subjects). Phase synchrony, another possible mechanism underlying functional connectivity, was also not investigated in this work but remains an interesting research topic.

Recent comparisons between MEG evoked responses and fMRI blood-oxygen-level-dependent signals point to reasonable similarities but also marked spatial and functional differences (Liljeström et al. 2009; Vartiainen et al. 2011). With MEG on humans, a complex relationship between alpha, beta and gamma band modulations and BOLD responses has been shown (Singh et al. 2002; Brookes et al. 2005; Winterer et al. 2007; Muthukumaraswamy and Singh 2009). In PIV, with partly the same data set as in the MEG-fMRI comparison study by Liljeström et al. 2009, the spatially convergent active brain areas found with rhythms and

evoked responses correspond quite well with the fMRI results of the same subjects. However, some studies indicate that fMRI might miss evoked responses of short duration (Furey et al. 2006). It is possible that a combination of evoked responses and rhythmic activity could lead to a better model for linking EEG/MEG and fMRI than either measure alone (Robitaille et al. 2010).

Connectivity estimation between brain regions is a particularly interesting application of DICS and erDICS. This is still a fairly new line of research in neuroscience that holds great promise. Besides coherence, information transfer between cortical areas could manifest in the form of cross-frequency coupling (CFC), i.e., coupling between the phase of low frequency rhythms and the power of high frequency rhythms. Intracranial recordings have suggested that CFC plays a role in coordination between cortical areas (Canolty et al. 2006) and working memory (Axmacher et al. 2010), and MEG measurements have linked CFC with functional integration of spectrally-distributed processing (Palva et al. 2005) and enhancement of weak signal detection (Händel and Haarmeier 2009). CFC could be implemented with DICS/erDICS, for example, by extracting time series for different frequency bands with the beamformer and then performing CFC analysis between all grid points. This would allow DICS/erDICS to quantify the potentially important cross-frequency interplay in the brain.

Bibliography

Axmacher, N., Henseler, M.M., Jensen, O., Weinreich, I., Elger, C.E., Fell, J., 2010. Cross-frequency coupling supports multi-item working memory in the human hippocampus. *Proc Natl Acad Sci U S A* 107:3228–3233.

Barnes, G.R., Hillebrand, A., 2003. Statistical flattening of MEG beamformer images. *Hum Brain Mapp* 18:1–12.

Berger, H., 1929. Über das Elektroenkephalogramm des Menschen. *Arch Psychiatr Nervenkr* 87:527–570.

Brenner, D., Lipton, J., Kaufman, L., Williamson, S.J., 1978. Somatically evoked magnetic fields of the human brain. *Science* 199:81–83.

Brenner, D., Williamson, S.J., Kaufman, L., 1975. Visually evoked magnetic fields of the human brain. *Science* 190:480–482.

Brookes, M.J., Gibson, A.M., Hall, S.D., Furlong, P.L., Barnes, G.R., Hillebrand, A., Singh, K.D., Holliday, I.E., Francis, S.T., Morris, P.G., 2005. GLM-beamformer method demonstrates stationary field, alpha ERD and gamma ERS co-localisation with fMRI BOLD response in visual cortex. *Neuroimage* 26:302–308.

Büchel, C., Friston, K.J., 1997. Modulation of connectivity in visual pathways by attention: cortical interactions evaluated with structural equation modelling and fMRI. *Cereb Cortex* 7:768–778.

Canolty, R.T., Edwards, E., Dalal, S.S., Soltani, M., Nagarajan, S.S., Kirsch, H.E., Berger, M.S., Barbaro, N.M., Knight, R.T., 2006. High gamma power is phase-locked to theta oscillations in human neocortex. *Science* 313:1626–1628.

Chen, R., Yaseen, Z., Cohen, L.G., Hallett, M., 1998. Time course of corticospinal excitability in reaction time and self-paced movements. *Ann Neurol* 44:317–325.

Cohen, D., 1968. Magnetoencephalography: evidence of magnetic fields produced by alpha-rhythm currents. *Science* 161:784–786.

Cohen, D., 1972. Magnetoencephalography: detection of the brain's electrical activity with a superconducting magnetometer. *Science* 175:664–666.

Crouzeix, A., Yvert, B., Bertrand, O., Pernier, J., 1999. An evaluation of dipole reconstruction accuracy with spherical and realistic head models in MEG. *Clin Neurophysiol* 110:2176–2188.

Dahlhaus, R., Eichler, M., Sandkühler, J., 1997. Identification of synaptic connections in neural ensembles by graphical models. *J Neurosci Methods* 77:93–107.

DeLeon, J., Gottesman, R.F., Kleinman, J.T., Newhart, M., Davis, C., Heidler-Gary, J., Lee, A., Hillis, A.E., 2007. Neural regions essential for distinct cognitive processes underlying picture naming. *Brain* 130:1408–1422.

Desikan, R.S., Segonne, F., Fischl, B., Quinn, B.T., Dickerson, B.C., Blacker, D., Buckner, R.L., Dale, A.M., Maguire, R.P., Hyman, B.T., Albert, M.S., Killiany, R.J., 2006. An automated labeling system for subdividing the human cerebral cortex on MRI scans into gyral based regions of interest. *Neuroimage* 31:968–980.

Dinse, H.R., Kruger, K., Akhavan, A.C., Spengler, F., Schoner, G., Schreiner, C.E., 1997. Low-frequency oscillations of visual, auditory and somatosensory cortical neurons evoked by sensory stimulation. *Int J Psychophysiol* 26:205–227.

Fischl, B., van der Kouwe, A., Destrieux, C., Halgren, E., Segonne, F., Salat, D.H., Busa, E., Seidman, L.J., Goldstein, J., Kennedy, D., Caviness, V., Makris, N., Rosen, B., Dale, A.M., 2004. Automatically parcellating the human cerebral cortex. *Cereb Cortex* 14:11–22.

Fries, P., Reynolds, J.H., Rorie, A.E., Desimone, R., 2001. Modulation of oscillatory neuronal synchronization by selective visual attention. *Science* 291:1560–1563.

Furey, M.L., Tanskanen, T., Beauchamp, M.S., Avikainen, S., Uutela, K., Hari, R., Haxby, J.V., 2006. Dissociation of face-selective cortical responses by attention. *Proc Natl Acad Sci U S A* 103:1065–1070.

Gastaut, H., 1952. [Electrocorticographic study of the reactivity of rolandic rhythm]. *Rev Neurol (Paris)* 87:176–182.

Geweke, J., 1982. Measurement of Linear Dependence and Feedback Between Multiple Time Series. *J Amer Statistical Assoc* 77:304–313.

Granger, C., 1980. Testing for causality: a personal viewpoint. *J Econ Dyn Control* 2:329–352.

Gross, J., Ioannides, A.A., 1999. Linear transformations of data space in MEG. *Phys Med Biol* 44:2081–2097.

Gross, J., Kujala, J., Hämäläinen, M., Timmermann, L., Schnitzler, A., Salmelin, R., 2001. Dynamic imaging of coherent sources: Studying neural interactions in the human brain. *Proc Natl Acad Sci U S A* 98:694–699.

Guo, S., Seth, A.K., Kendrick, K.M., Zhou, C., Feng, J., 2008. Partial Granger causality–eliminating exogenous inputs and latent variables. *J Neurosci Methods* 172:79–93.

Hämäläinen, M., Hari, R., Ilmoniemi, R.J., Knuutila, J., Lounasmaa, O.V., 1993. Magnetoencephalography - Theory, Instrumentation, and Applications to Noninvasive Studies of the Working Human Brain. *Rev Mod Phys* 65:413–497.

Hämäläinen, M.S., Ilmoniemi, R.J., 1994. Interpreting magnetic fields of the brain: minimum norm estimates. *Med Biol Eng Comput* 32:35–42.

Hämäläinen, M.S., Sarvas, J., 1989. Realistic conductivity geometry model of the human head for interpretation of neuromagnetic data. *IEEE Trans Biomed Eng* 36:165–171.

Händel, B., Haarmeier, T., 2009. Cross-frequency coupling of brain oscillations indicates the success in visual motion discrimination. *Neuroimage* 45:1040–1046.

Hansen, P., Kringelbach, M., Salmelin, R. (editors), 2010. MEG: An introduction to methods. Oxford University Press.

Hari, R., Aittoniemi, K., Järvinen, M.L., Katila, T., Varpula, T., 1980. Auditory evoked transient and sustained magnetic fields of the human brain. Localization of neural generators. *Exp Brain Res* 40:237–240.

Hari, R., Salmelin, R., 1997. Human cortical oscillations: a neuromagnetic view through the skull. *Trends Neurosci* 20:44–49.

Helenius, P., Salmelin, R., Service, E., Connolly, J.F., 1998. Distinct time courses of word and context comprehension in the left temporal cortex. *Brain* 121:1133–1142.

Henery, C.C., Mayhew, T.M., 1989. The cerebrum and cerebellum of the fixed human brain: efficient and unbiased estimates of volumes and cortical surface areas. *J Anat* 167:167–180.

Hillebrand, A., Barnes, G.R., 2002. A quantitative assessment of the sensitivity of whole-head MEG to activity in the adult human cortex. *Neuroimage* 16:638–650.

Hillebrand, A., Singh, K.D., Holliday, I.E., Furlong, P.L., Barnes, G.R., 2005. A new approach to neuroimaging with magnetoencephalography. *Hum Brain Mapp* 25:199–211.

Holmes, A.P., Blair, R.C., Watson, J.D., Ford, I., 1996. Nonparametric analysis of statistic images from functional mapping experiments. *J Cereb Blood Flow Metab* 16:7–22.

Hoogenboom, N., Schoffelen, J.M., Oostenveld, R., Parkes, L.M., Fries, P., 2006. Localizing human visual gamma-band activity in frequency, time and space. *Neuroimage* 29:764–773.

Huang, C.S., Hiraba, H., Sessle, B.J., 1989. Input-output relationships of the primary face motor cortex in the monkey (Macaca fascicularis). *J Neurophysiol* 61:350–362.

Hultén, A., Vihla, M., Laine, M., Salmelin, R., 2009. Accessing newly learned names and meanings in the native language. *Hum Brain Mapp* 30:976–989.

Indefrey, P., Levelt, W.J., 2004. The spatial and temporal signatures of word production components. *Cognition* 92:101–144.

Ishii, R., Shinosaki, K., Ukai, S., Inouye, T., Ishihara, T., Yoshimine, T., Hirabuki, N., Asada, H., Kihara, T., Robinson, S.E., Takeda, M., 1999. Medial prefrontal cortex generates frontal midline theta rhythm. *Neuroreport* 10:675–679.

Jensen, O., Gelfand, J., Kounios, J., Lisman, J.E., 2002. Oscillations in the alpha band (9-12 Hz) increase with memory load during retention in a short-term memory task. *Cereb Cortex* 12:877–882.

Jensen, O., Tesche, C.D., 2002. Frontal theta activity in humans increases with memory load in a working memory task. *Eur J Neurosci* 15:1395–1399.

Josephson, B., 1962. Possible new effects in superconductive tunnelling. *Phys Lett* 1:251–253.

Karhu, J., Hari, R., Lu, S.T., Paetau, R., Rif, J., 1991. Cerebral magnetic fields to lingual stimulation. *Electroencephalogr Clin Neurophysiol* 80:459–468.

Kello, C.T., Brown, G.D.A., Ferrer-I-Cancho, R., Holden, J.G., Linkenkaer-Hansen, K., Rhodes, T., Van Orden, G.C., 2010. Scaling laws in cognitive sciences. *Trends Cogn Sci* 14:223–232.

Lachaux, J.P., Rodriguez, E., Martinerie, J., Varela, F.J., 1999. Measuring phase synchrony in brain signals. *Hum Brain Mapp* 8:194–208.

Leahy, R.M., Mosher, J.C., Spencer, M.E., Huang, M.X., Lewine, J.D., 1998. A study of dipole localization accuracy for MEG and EEG using a human skull phantom. *Electroencephalogr Clin Neurophysiol* 107:159–173.

Liljeström, M., Hultén, A., Parkkonen, L., Salmelin, R., 2009. Comparing MEG and fMRI views to naming actions and objects. *Hum Brain Mapp* 30:1845–1856.

Linkenkaer-Hansen, K., Nikouline, V.V., Palva, J.M., Ilmoniemi, R.J., 2001. Long-range temporal correlations and scaling behavior in human brain oscillations. *J Neurosci* 21:1370–1377.

Logothetis, N.K., 2003. MR imaging in the non-human primate: studies of function and of dynamic connectivity. *Curr Opin Neurobiol* 13:630–642.

Mahon, B.Z., Caramazza, A., 2009. Concepts and categories: a cognitive neuropsychological perspective. *Annu Rev Psychol* 60:27–51.

Makeig, S., Westerfield, M., Jung, T.P., Enghoff, S., Townsend, J., Courchesne, E., Sejnowski, T.J., 2002. Dynamic brain sources of visual evoked responses. *Science* 295:690–694.

Mäkinen, V., Tiitinen, H., May, P., 2005. Auditory event-related responses are generated independently of ongoing brain activity. *Neuroimage* 24:961–968.

Marinkovic, K., Dhond, R.P., Dale, A.M., Glessner, M., Carr, V., Halgren, E., 2003. Spatiotemporal dynamics of modality-specific and supramodal word processing. *Neuron* 38:487–497.

Maris, E., Oostenveld, R., 2007. Nonparametric statistical testing of EEG- and MEG-data. *J Neurosci Methods* 164:177–190.

Matsuura, K., Okabe, Y., 1995. Selective minimum-norm solution of the biomagnetic inverse problem. *IEEE Trans Biomed Eng* 42:608–615.

Mazaheri, A., Jensen, O., 2006. Posterior alpha activity is not phase-reset by visual stimuli. *Proc Natl Acad Sci U S A* 103:2948–2952.

Mazaheri, A., Jensen, O., 2008. Asymmetric amplitude modulations of brain oscillations generate slow evoked responses. *J Neurosci* 28:7781–7787.

Mechelli, A., Price, C.J., Friston, K.J., Ishai, A., 2004. Where bottom-up meets top-down: neuronal interactions during perception and imagery. *Cereb Cortex* 14:1256–1265.

Montez, T., Poil, S.S., Jones, B.F., Manshanden, I., Verbunt, J.P.A., van Dijk, B.W., Brussaard, A.B., van Ooyen, A., Stam, C.J., Scheltens, P., Linkenkaer-Hansen, K., 2009. Altered temporal correlations in parietal alpha and prefrontal theta oscillations in early-stage Alzheimer disease. *Proc Natl Acad Sci U S A* 106:1614–1619.

Morlet, J., Arens, G., Fourgeau, E., Giard, D., 1982. Wave propagation and sampling theory - Part I: Complex signal and scattering in multilayered media. *Geophys* 41:203–221.

Muthukumaraswamy, S.D., Singh, K.D., 2009. Functional decoupling of BOLD and gamma-band amplitudes in human primary visual cortex. *Hum Brain Mapp* 30:2000–2007.

Muthukumaraswamy, S.D., Singh, K.D., Swettenham, J.B., Jones, D.K., 2010. Visual gamma oscillations and evoked responses: variability, repeatability and structural MRI correlates. *Neuroimage* 49:3349–3357.

Nichols, T.E., Holmes, A.P., 2002. Nonparametric permutation tests for functional neuroimaging: a primer with examples. *Hum Brain Mapp* 15:1–25.

Niedermeyer, E., 1990. Alpha-like rhythmical activity of the temporal lobe. *Clin Electroencephalogr* 21:210–224.

Nikulin, V.V., Linkenkaer-Hansen, K., Nolte, G., Lemm, S., Müller, K.R., Ilmoniemi, R.J., Curio, G., 2007. A novel mechanism for evoked responses in the human brain. *Eur J Neurosci* 25:3146–3154.

Nobre, A.C., McCarthy, G., 1994. Language-related ERPs: scalp distributions and modulation by word type and semantic priming. *J Cogn Neurosci* 6:233–255.

Nunez, P.L., Srinivasan, R., Westdorp, A.F., Wijesinghe, R.S., Tucker, D.M., Silberstein, R.B., Cadusch, P.J., 1997. EEG coherency. I: Statistics, reference electrode, volume conduction, Laplacians, cortical imaging, and interpretation at multiple scales. *Electroencephalogr Clin Neurophysiol* 103:499–515.

Okada, Y.C., Wu, J., Kyuhou, S., 1997. Genesis of MEG signals in a mammalian CNS structure. *Electroencephalogr Clin Neurophysiol* 103:474–485.

Palva, J.M., Palva, S., Kaila, K., 2005. Phase synchrony among neuronal oscillations in the human cortex. *J Neurosci* 25:3962–3972.

Penfield, W., Boldrey, E., 1937. Somatic motor and sensory representaion in the cerebral cortex of man as studied by electrical stimulation. *Brain* 60:389–443.

Penny, W.D., Stephan, K.E., Mechelli, A., Friston, K.J., 2004. Modelling functional integration: a comparison of structural equation and dynamic causal models. *Neuroimage* 23 Suppl 1:S264–S274.

Pfurtscheller, G., 1981. Central beta rhythm during sensorimotor activities in man. *Electroencephalogr Clin Neurophysiol* 51:253–264.

Pfurtscheller, G., Lopes da Silva, F.H., 1999. Event-related EEG/MEG synchronization and desynchronization: basic principles. *Clin Neurophysiol* 110:1842–1857.

Robinson, S.E., Vrba, J., 1999. Functional neuroimaging by synthetic aperture magnetometry (SAM). In Biomag, pages 302–305. Tohoku University Press, Sendai.

Robitaille, N., Marois, R., Todd, J., Grimault, S., Cheyne, D., Jolicoeur, P., 2010. Distinguishing between lateralized and nonlateralized brain activity associated with visual short-term memory: fMRI, MEG, and EEG evidence from the same observers. *Neuroimage* 53:1334–1345.

Roland, P.E., Zilles, K., 1996. The developing European computerized human brain database for all imaging modalities. *Neuroimage* 4:S39–47.

Rosenblum, M.G., Pikovsky, A.S., 2001. Detecting direction of coupling in interacting oscillators. *Phys Rev E* 64:045202.

Rossell, S.L., Price, C.J., Nobre, A.C., 2003. The anatomy and time course of semantic priming investigated by fMRI and ERPs. *Neuropsychologia* 41:550–564.

Salenius, S., Kajola, M., Thompson, W.L., Kosslyn, S., Hari, R., 1995. Reactivity of magnetic parieto-occipital alpha rhythm during visual imagery. *Electroencephalogr Clin Neurophysiol* 95:453–462.

Salmelin, R., 2007. Clinical neurophysiology of language: the MEG approach. *Clin Neurophysiol* 118:237–254.

Salmelin, R., Hämäläinen, M., Kajola, M., Hari, R., 1995. Functional segregation of movement-related rhythmic activity in the human brain. *Neuroimage* 2:237–243.

Salmelin, R., Hari, R., 1994a. Characterization of spontaneous MEG rhythms in healthy adults. *Electroencephalogr Clin Neurophysiol* 91:237–248.

Salmelin, R., Hari, R., 1994b. Spatiotemporal characteristics of sensorimotor neuromagnetic rhythms related to thumb movement. *Neuroscience* 60:537–550.

Salmelin, R., Hari, R., Lounasmaa, O.V., Sams, M., 1994. Dynamics of brain activation during picture naming. *Nature* 368:463–465.

Salmelin, R., Sams, M., 2002. Motor cortex involvement during verbal versus non-verbal lip and tongue movements. *Hum Brain Mapp* 16:81–91.

Salmelin, R., Schnitzler, A., Schmitz, F., Freund, H.J., 2000. Single word reading in developmental stutterers and fluent speakers. *Brain* 123:1184–1202.

Salmelin, R.H., Hämäläinen, M.S., 1995. Dipole modelling of MEG rhythms in time and frequency domains. *Brain Topogr* 7:251–257.

Sameshima, K., Baccala, L.A., 1999. Using partial directed coherence to describe neuronal ensemble interactions. *J Neurosci Methods* 94:93–103.

Sarvas, J., 1987. Basic mathematical and electromagnetic concepts of the biomagnetic inverse problem. *Phys Med Biol* 32:11–22.

Schnitzler, A., Salenius, S., Salmelin, R., Jousmäki, V., Hari, R., 1997. Involvement of primary motor cortex in motor imagery: a neuromagnetic study. *Neuroimage* 6:201–208.

Schormann, T., Henn, S., Zilles, K., 1996. A new approach to fast elastic alignment with applications to human brains. *Lecture Notes Comput Sci* 1131:337–342.

Sekihara, K., Nagarajan, S.S., Poeppel, D., Marantz, A., 2002. Performance of an MEG adaptive-beamformer technique in the presence of correlated neural activities: effects on signal intensity and time-course estimates. *IEEE Trans Biomed Eng* 49:1534–1546.

Shah, A.S., Bressler, S.L., Knuth, K.H., Ding, M., Mehta, A.D., Ulbert, I., Schroeder, C.E., 2004. Neural dynamics and the fundamental mechanisms of event-related brain potentials. *Cereb Cortex* 14:476–483.

Simos, P.G., Basile, L.F., Papanicolaou, A.C., 1997. Source localization of the N400 response in a sentence-reading paradigm using evoked magnetic fields and magnetic resonance imaging. *Brain Res* 762:29–39.

Singer, W., 1999. Neuronal synchrony: a versatile code for the definition of relations? *Neuron* 24:49–65, 111–125.

Singer, W., Gray, C.M., 1995. Visual feature integration and the temporal correlation hypothesis. *Annu Rev Neurosci* 18:555–586.

Singh, K.D., Barnes, G.R., Hillebrand, A., Forde, E.M., Williams, A.L., 2002. Task-related changes in cortical synchronization are spatially coincident with the hemodynamic response. *Neuroimage* 16:103–114.

Tallon-Baudry, C., Bertrand, O., Delpuech, C., Permier, J., 1997. Oscillatory gamma-band (30-70 Hz) activity induced by a visual search task in humans. *J Neurosci* 17:722–734.

Tarkiainen, A., Liljestrom, M., Seppä, M., Salmelin, R., 2003. The 3D topography of MEG source localization accuracy: effects of conductor model and noise. *Clin Neurophysiol* 114:1977–1992.

Tass, P., Rosenblum, M., Weule, J., Kurths, J., Pikovsky, A., Volkmann, J., Schnitzler, A., Freund, H.J., 1998. Detection of n:m phase locking from noisy data: application to magnetoencephalography. *Phys Rev Lett* 81:3291–3294.

Taulu, S., Kajola, M., Simola, J., 2004. Suppression of interference and artifacts by the Signal Space Separation Method. *Brain Topogr* 16:269–275.

Tiihonen, J., Hari, R., Kajola, M., Karhu, J., Ahlfors, S., Tissari, S., 1991. Magnetoencephalographic 10-Hz rhythm from the human auditory cortex. *Neurosci Lett* 129:303–305.

Tuladhar, A.M., ter Huurne, N., Schoffelen, J.M., Maris, E., Oostenveld, R., Jensen, O., 2007. Parieto-occipital sources account for the increase in alpha activity with working memory load. *Hum Brain Mapp* 28:785–792.

Uusitalo, M.A., Ilmoniemi, R.J., 1997. Signal-space projection method for separating MEG or EEG into components. *Med Biol Eng Comput* 35:135–140.

Uusvuori, J., Parviainen, T., Inkinen, M., Salmelin, R., 2008. Spatiotemporal interaction between sound form and meaning during spoken word perception. *Cereb Cortex* 18:456–466.

Uutela, K., Hämäläinen, M., Somersalo, E., 1999. Visualization of magnetoencephalographic data using minimum current estimates. *Neuroimage* 10:173–180.

van Dijk, H., van der Werf, J., Mazaheri, A., Medendorp, W.P., Jensen, O., 2010. Modulations in oscillatory activity with amplitude asymmetry can produce cognitively relevant event-related responses. *Proc Natl Acad Sci U S A* 107:900–905.

Van Veen, B., Buckley, K., 1988. Beamforming: a versatile approach to spatial filtering. *IEEE ASSP Magazine* 5:4–24.

Van Veen, B.D., van Drongelen, W., Yuchtman, M., Suzuki, A., 1997. Localization of brain electrical activity via linearly constrained minimum variance spatial filtering. *IEEE Trans Biomed Eng* 44:867–880.

Vanni, S., Revonsuo, A., Hari, R., 1997. Modulation of the parieto-occipital alpha rhythm during object detection. *J Neurosci* 17:7141–7147.

Vanni, S., Revonsuo, A., Saarinen, J., Hari, R., 1996. Visual awareness of objects correlates with activity of right occipital cortex. *Neuroreport* 8:183–186.

Varela, F., Lachaux, J.P., Rodriguez, E., Martinerie, J., 2001. The brainweb: phase synchronization and large-scale integration. *Nat Rev Neurosci* 2:229–239.

Vartiainen, J., Liljeström, M., Koskinen, M., Renvall, H., Salmelin, R., 2011. Functional magnetic resonance imaging blood oxygenation level-dependent signal and magnetoencephalography evoked responses yield different neural functionality in reading. *J Neurosci* 31:1048–1058.

Vartiainen, J., Parviainen, T., Salmelin, R., 2009. Spatiotemporal convergence of semantic processing in reading and speech perception. *J Neurosci* 29:9271–9280.

Vihla, M., Laine, M., Salmelin, R., 2006. Cortical dynamics of visual/semantic vs. phonological analysis in picture confrontation. *Neuroimage* 33:732–738.

Welch, P., 1967. The use of fast Fourier transform for the estimation of power spectra: A method based on time averaging over short, modified periodograms. *IEEE Trans Audio* 15:70–73.

Winterer, G., Carver, F.W., Musso, F., Mattay, V., Weinberger, D.R., Coppola, R., 2007. Complex relationship between BOLD signal and synchronization/desynchronization of human brain MEG oscillations. *Hum Brain Mapp* 28:805–816.

Woods, R.P., Grafton, S.T., Holmes, C.J., Cherry, S.R., Mazziotta, J.C., 1998a. Automated image registration: I. General methods and intrasubject, intramodality validation. *J Comput Assist Tomogr* 22:139–152.

Woods, R.P., Grafton, S.T., Watson, J.D., Sicotte, N.L., Mazziotta, J.C., 1998b. Automated image registration: II. Intersubject validation of linear and nonlinear models. *J Comput Assist Tomogr* 22:153–165.

Wydell, T.N., Vuorinen, T., Helenius, P., Salmelin, R., 2003. Neural correlates of letter-string length and lexicality during reading in a regular orthography. *J Cogn Neurosci* 15:1052–1062.

Zhang, J., Riehle, A., Requin, J., Kornblum, S., 1997. Dynamics of single neuron activity in monkey primary motor cortex related to sensorimotor transformation. *J Neurosci* 17:2227–2246.

Zimmerman, J., Silver, A.H., 1966. Macroscopic Quantum Interference Effects through Superconducting Point Contacts. *Phys Rev* 141:367–375.

Zimmerman, J., Thiene, P., Harding, J.T., 1970. Design and Operation of Stable Rf-Biased Superconducting Point-Contact Quantum Devices, and a Note on Properties of Perfectly Clean Metal Contacts. *J Appl Phys* 41:1572–1580.

Aalto-DD 119/2012

ISBN 978-952-60-4786-7
ISBN 978-952-60-4787-4 (pdf)
ISSN-L 1799-4934
ISSN 1799-4934
ISSN 1799-4942 (pdf)

Aalto University
School Of Science
Brain Research Unit, O.V. Lounasmaa Laboratory
www.aalto.fi

BUSINESS +
ECONOMY

ART +
DESIGN +
ARCHITECTURE

SCIENCE +
TECHNOLOGY

CROSSOVER

**DOCTORAL
DISSERTATIONS**